January 2011

Platelet Induction Of Monocyte To Dendritic Cell Differentiation

Tyler Durazzo
Yale School of Medicine, tyler.durazzo@gmail.com

Platelet Induction of Monocyte to Dendritic Cell Differentiation

A Thesis Submitted to the

Yale University School of Medicine

In Partial Fulfillment of the Requirements for the

Degree of Doctor of Medicine

By

Tyler S. Durazzo

2011

PLATELET INDUCTION OF MONOCYTE TO DENDRITIC CELL DIFFERENTIATION. Tyler S. Durazzo, Robert E Tigelaar, Carole L Berger, Michael Girardi, Richard L Edelson. Department of Dermatology, Yale Cancer Center, Yale University, School of Medicine, New Haven, CT

We hypothesized that activated platelets induce monocyte-to-dendritic cell (DC) differentiation. The aims of this study were to: (1) determine the role that platelets play, if any, in the signaling of monocyte to DC differentiation; (2) determine the mechanism of action by which platelets induce monocyte-to-DC differentiation. (3) Use this knowledge to advance cancer immunotherapy.

To achieve these ends: (1) parallel-plate flow chambers were designed to deliver monocytes a controlled level of platelet exposure, with phenotype and genotype assessed following overnight incubation; (2) blocking antibodies and proteins were used to assess for the significance of particular monocyte-platelet interactions in the mechanism; (3) additional experiments and mathematical modeling was performed to extrapolate our new mechanistic knowledge to enhance extracorporeal photochemotherapy (ECP), an immunotherapy in clinical use.

Results showed direct correlation between platelet exposure and level of DC differentiation following overnight incubation ($p < 0.0001$). A detailed mechanism was determined involving p-selectin and other proteins expressed by activated platelets. This mechanistic knowledge permitted intelligent modification of ECP.

We conclude that platelets induce monocyte to DC differentiation. The rapidity and efficiency of this induction suggests the possibility that this is a physiologic mechanism employed in-vivo for DC differentiation. Possible exploitation of this mechanism may prove beneficial in cancer immunotherapy.

ACKNOWLEDGEMENTS

This thesis was possible thanks to the help and guidance of several individuals:

First and foremost, I would like to thank Dr. Richard Edelson for his mentorship; one could not ask for a better mentor or model in academic medicine, he has far exceeded that of any individual I've come in contact with previously. Neither my interactions with him nor his dedication to my career development will ever be forgotten.

Dr. Robert Tigelaar, for his expertise in immunobiology and critical evaluation of the work. His availability to always enthusiastically discuss and critique my latest data and ideas was extremely valuable.

Dr. Carole Berger, for her award-winning research which provided much of the foundation leading to the hypothesis in this thesis; as well as for her day-to-day support in lab.

Dr. Michael Girardi for his research expertise and helpful words of wisdom during monthly lab meetings.

Mae Geter and Donna Carranzo for going beyond what was required of them to make sure I had research funding; Dr. Forrest, the Office of Student Research, the NIH, NY Cardiac Foundation, and Yale SPORE in Skin Cancer for providing the funding necessary for this work.

And last but not least, my mom for supporting me throughout my time in college and medical school, and for being proud of me long before there were tangible things to be proud of.

TABLE OF CONTENTS

1. INTRODUCTION

1.1 Overview

Due to high response rates and an excellent safety profile, extracorporeal photochemotherapy (ECP) is widely used for immunotherapy in patients with leukemic cutaneous T-cell lymphoma (CTCL), graft versus host disease, and organ transplant rejection [1]. Recently, it has been reported that ECP induces a high percentage of processed monocytes to enter the dendritic cell (DC) differentiation pathway, within a single day of treatment [2]. Despite intense research, the mechanism by which ECP induces this differentiation has remained elusive.

Dendritic cells (DC) are the most potent antigen presenting cells in the human body, orders of magnitude more powerful than any other cell type know [3]. Their physiologic role has proven to be central to immune function. Located at the interface between innate and adaptive immunity, DC orchestrate the immune system's response via their influence on CD4+ T-cells, CD8+ T-cells, and other effector cell types [4]. Their central role in the immune system has recently placed them at the forefront of cancer immunotherapy [5-7].

We investigated the mechanism by which ECP induces monocyte-to-DC differentiation. The efficiency and rapidity of this cellular conversion, occurring without addition of exogenous growth factors, suggests that the manner in which ECP induces monocytes to differentiate into DC may result from the co-opting of a normal physiologic mechanism controlling DC maturation. Hence, elucidation of the

molecular basis for ECP's influence on monocytes may provide important clues about in-vivo DC generation.

To investigate this phenomenon, we developed an ECP model which could be visualized with digital microscopy and therefore permit direct visualization of the cellular components and flow dynamics involved. We report in this thesis that activated platelets induce monocyte-to-DC differentiation under flow conditions mimicking those found in post-capillary venules.

1.2 Physiologic Dendritic Cell Development

Relatively little is known regarding DC development in comparison to other cells of haemotopoietic origin. Based on evidence mainly from mouse models, current theories propose that most DC develop in vivo from hematopoietic stem cell-derived progenitors with both lymphoid and myeloid-restricted differentiation potential [8]. One common precursor is believed to give rise to monocytes, macrophages, and dendritic cells in the bone marrow. Furthermore, some monocytes possess the potential, after leaving the bone marrow, to differentiate under inflammatory conditions into both DC and macrophages [9]. It is this DC differentiation from peripheral blood monocytes which is of particular relevance to this thesis.

Much work remains to be done in terms of elucidating the in-vivo factors responsible for inducing peripheral blood monocyte-to-dendritic cell differentiation. Part of the difficulty in the field has stemmed from the complexity and varying nature of

monocyte populations, as well as inconsistencies among studies done in-vivo versus in-vitro [9-11]. These inconsistencies, however, have drawn attention to the likelihood that physiologic monocyte-to-DC differentiation in-vivo is dependent on both intrinsic monocyte potential as well as factors acting upon the monocyte.

There exists clear evidence that human blood monocytes are heterogeneous: expressing different proteins, responding differently to various stimuli, and producing different products [11]. In vivo studies have provided evidence that two monocyte subpopulations, Ly6C+ and Ly6C-, apparently have separate potentials, regardless of the factors acting upon them [12-15]. Ly6C+ monocytes appear capable of differentiation into DC, Langerhans cells, inflammatory macrophages, or myeloid-derived suppressor cells; Ly6C- monocytes appear to have the potential to differentiate into alveolar macrophages [9].

In vitro studies have provided evidence for environmental factors that contribute to DC differentiation. Exposing both human and mouse monocytes to suprapharmacologic doses of IL-4 and GM-CSF for long periods in culture results in differentiation into DC, regardless of the monocyte subset [10, 16, 17]. Furthermore, addition of TGF-β1 to the cultures results in Langerhans cell differentiation [18]. In contrast, addition of IL-6 to the same cultures results in macrophage, not DC, differentiation [19]. Exposing monocytes to M-CSF in vitro also results in macrophage differentiation [18]. Monocytes cultured with M-CSF can be further influenced to differentiate into either

M1 or M2-subtype macrophages by addition of either IFN-gamma or IL-4, respectively [20, 21].

It is clear that in vitro, monocyte differentiation is influenced heavily by the cytokine environment, albeit only to suprapharmacologic doses. How to precisely extrapolate these findings to physiologic in-vivo mechanisms of monocyte-to-DC differentiation remains to be determined. Additionally, functional differences between those in-vitro generated cells and their in-vivo counterparts have not yet been fully explored. As outlined in section 1.4, DC generated using in-vitro suprapharmacologic cytokines have been relatively unsuccessful at reaching the theoretical potential DC posses in cancer immunotherapy.

1.3 Extracorporeal Photochemotherapy (ECP)

ECP is the first FDA approved cellular immunotherapy, originally introduced in 1987 for the treatment of patients with severe CTCL [22]. Since its initial introduction, the therapy's clinical application has been extended to include successful treatment of patients with chronic graft-versus host disease (GVHD), and prevention of organ transplant rejection [23, 24]. The therapy's high clinical success rate in otherwise therapeutically resistant situations, in addition to its low toxicity [25], has led to the therapy being used over 1.5 million times in over 150 centers throughout the world. Despite the therapy's clinical success, its precise mechanism of action has remained unknown. Recent studies have shown that the therapy causes monocyte-to-DC

differentiation, however the mechanism responsible for this induction remains unidentified [1, 2].

The therapy consists of collecting a small number (<10%) of a patient's lymphocytes via leukophersis of peripheral blood. 8-methoxypsoralen (8-MOP) is then added to these collected cells (suspended in plasma), followed by passage of the cells through a 1-mm space located between two transparent plastic plates. While the cells are passed through the transparent plates, they are irradiated with UVA energy, causing 8-MOP to become activated and covalently crosslink thymine bases of DNA [26]; this crosslinking causes a fraction of cells to undergo apoptosis. The therapy is completed by reinfusing the treated cells into the patient.

Interestingly, the treatment is conducted identically as described for both CTCL (a cancer expected to respond to immunostimulation), as well as GVHD (a condition expected to positively respond to immunosuppression). The seemingly paradoxical ability of the same treatment to invoke immunotherapeutic responses at both ends of the spectrum is consistent with ability of the treatment to generate fully functional dendritic cells; dendritic cells are well known for their physiologic capacity to orchestrate immune responses in either direction, depending on stimuli encountered in the body [4].

The DCs generated by ECP have been shown to be functionally capable of processing and presenting exogenous and endogenous antigen [2]. Furthermore, microarray

analysis have shown that ECP-processed monocytes show expression profiles consistent with functional DC, with up or down regulation of more than 1100 genes [2]. Dramatic increases in surface expression of proteins critical to DC function have also been documented in DC generated by ECP. Interestingly, all these changes described occur in less than 18 hours after treatment, without the need for any exogenous cytokines or growth factors.

The time course of DC induction, the non-requirement for exogenous growth factors, and the clinical success, all suggest that the ECP may be recapitulating a physiologic mechanism of DC generation. Therefore, study of ECP's unknown mechanism of DC induction may provide insight into physiologic principles of DC generation. Furthermore, if these principles are uncovered, improvements to the ECP system may be made which allow for better control, greater influence, and higher DC yields.

1.4 Dendritic Cells and Cancer Immunotherapy

DCs' central role in the immune system has placed them at the forefront of cancer immunotherapy. Recent years have seen an increase in attempts at generating DC for the purpose of inducing clinical immunity against various cancers [5-7]. These therapeutic protocols have thus far not lived up to the theoretical potential DCs possess. One potential explanation for the relative lack of successes is that the vast majority of protocols are based on generating DC from monocytes by administering suprapharmacologic doses of cytokines and growth factors, for instance, CM-CSF and IL-4 for 6 days, followed by TNF-alpha for 2 days [27]. As stated earlier, the

functional correspondence among DC generated in this manner in comparison to those generated physiologically is unknown. A better understanding of physiologic principles of DC generation may allow for their theoretical potential of generating cancer immunity to be better realized.

1.5 Platelets and Immunobiology

Platelets are well recognized for their main role in thrombus formation and maintenance of hemostasis. However, a comparatively recent body of literature has revealed an additional relevant function in immunobiology [28, 29].

Platelets are cell fragments derived from the cytoplasm of megakaryocytes in the bone marrow. While only approximately 2 microns in diameter, they circulate at levels of approximately 300,000/μl in healthy individuals, making their total volume greater than any other leukocyte subset [30]. In addition, due to physical properties of flow dynamics in blood vessels (see Appendix A), their relatively small size places them more proximal to the endothelium than any leukocyte population, making them ideal for immune surveillance.

Studies have shown that inflammation within tissue leads to an imbalance of procoagulant and anticoagulant properties of the local endothelium, resulting in platelet recruitment and activation [29]. For instance, one of the first pro-inflammatory cytokines released at sites of tissue infection is TNF-alpha; this molecule has been shown to inhibit synthesis of protein C [31], an anticoagulant protein, while

simultaneously inducing TF production on the endothelium [32]. This results in thrombin activation and fibrin formation, which in turn recruits and activates platelets. Interestingly, TNF-alpha concurrently causes nitric oxide (NO) release from endothelium [33]. NO is a potent inhibitor of platelet aggregation; thus, TNF-alpha is able to delicately recruit and activate platelets to sites of inflammation while simultaneously preventing thrombus formation, which would likely prove detrimental to leukocyte recruitment by limiting perfusion of the inflamed region.

Activated platelets have been found to express and secrete a number of ligands and substances capable of recruiting and activating leukocytes, including p-selectin [29], CD40L [34], IL-1B [35], CCL5, and CXCL4 [36]. Complex interactions among platelets and leukocytes have been found to contribute to various immune processes, including progression of atherosclerotic lesions [37], wound healing [38], and atopic dermatitis [30]. While the body of literature implementing platelets in key immunologic roles continues to mount, a role in inducing monocyte-to-DC differentiation has not been described to our knowledge.

HYPOTHESIS AND SPECIFIC AIMS

The initial aim of the work presented in this thesis was to determine the mechanism behind ECP's induction of monocyte to dendritic cell differentiation. As described in the results section, preliminary experiments suggested a role for platelets, subsequently leading to our main hypothesis: platelets induce monocyte-to-dendritic cell differentiation.

The subsequent aims of the work presented in this thesis were to: (1) determine the role that platelets play, if any, in the signaling of monocyte to dendritic cell differentiation; (2) determine the mechanism of action in which platelets induce monocyte-to-dendritic cell differentiation; and (3) use the mechanistic knowledge gained to intelligently advance ECP with the hope of potentially extending its scope in cancer immunotherapy.

METHODS

Statement of author's contribution: All work composing this thesis and presented in the subsequent sections was performed by the first author of the thesis.

Obtainment of leukocytes and platelets: All samples were acquired from young, healthy subjects not taking medication, including aspirin, known to influence platelet function. Samples were obtained under the guidelines of the Yale Human Investigational Review Board. Informed consent was provided according to the Declaration of Helsinki. Peripherial blood specimens were collected through a 19-gauge needle from the antecubital vein into syringes containing heparin, then layered on Ficoll-Hypaque (Gallard-Schlessinger, Carle Place, N.Y.). Following centrifugation at 180g, the interface containing the mononuclear leukocyte fraction was collected and washed twice in HBSS, then resuspended in RPMI-1640 medium (GIBCO) to a final concentration of $5 * 10^6$ mononuclear cells/ml. Experiments with the obtained cells were performed within one hour of being acquired.

Preparation of Platelet-rich-Plasma: Whole blood was centrifuged at 150 *g* for 15 min at room temperature. The platelet-rich-plasma (PRP) layer was collected and centrifuged at 900 *g* for 5 min, and the platelet pellet resuspended in RPMI 1640 to the desired concentration.

Preparation of Parallel-Plates: Two types of parallel-plate flow chambers were used to model the flow dynamics of ECP. Experiments involving the assessment of cell-phenotype post-flow were conducted using the larger Glycotech system (Glycotech,

Rockville, MD). This system consisted of a volumetric flow path measuring 20000 x 10000 x 254 microns (length x width x height). The bottom plate in this system was composed of a 15mm petri dish (BD Biosciences, Durham, NC) separated by a gasket and vacuum-connected to an acrylic flow deck, which formed the upper plate. For experiments requiring the plates to be pre-coated with platelets, prior to assembling the flow chamber, 20 drops of the desired concentration of PRP was placed in the center of the petri dish and platelets allowed to settle for 20 minutes at room temperature. The petri dish was washed with 2ml of RPMI twice, and the flow chamber then assembled.

For experiments not involving the collection and phenotyping of cells post-flow, Vena8 biochips (Cellix Ltd, Dublin, Ireland) were used to generate laminar flow. The volumetric flow path for a channel of the Vena8 biochips measured 20000 x 400 x 100 microns (length x width x height). Protein coating of these chips are described in the appropriate section below.

Experiments using Parallel-Plates: In all cases, the parallel-plate flow chamber was mounted on the stage of a phase contrast optical microscope (CK40, Olympus, Japan) with a 10x objective. All runs were performed at room temperature. A uniform laminar flow field was simulated by use of a syringe pump (KD Scientific, New Hope, PA) capable of generating near-constant volumetric flow rates. The components of the configuration were set up to minimize tubing. Prior to infusing cell suspensions through the plates, the configuration was washed with 5 ml of RPMI at a flow rate producing a wall shear stress of approximately 1 dyne/cm^2. Cell suspensions of

interest were then sent through the chamber at a fixed flow rate and wall shear stress (see Appendix A).

All experiments were viewed in real time while in progress, and recorded using a DP 200 digital camera and software (DeltaPix, Maalov, Denmark) at 15.2 frames per second. When applicable, images were analyzed using Image J software (NIH).

Overnight culture: When overnight culture was desired, cells were centrifuged and resuspended in RPMI-1640 medium (GIBCO), supplemented with 15% AB serum (Gemini Bio-Products) to a final concentration of 5 x 10E6 cells/ml. Cells were cultured overnight for 18 hours in 12-well polystyrene tissue culture pates (2 ml per well) at 37 degrees C with 5% CO2.

Immunophenotyping: Monoclonal antibodies for immunophenotyping included CD14 (LPS receptor; monocytes), CD11c (integrin subunit; monocytes and DC), HLA-DR (class II MHC molecule), CD83 (DC marker), CD62p (P-selectin; activated platelets), and CD61 (integrin subunit; platelets). Antibodies were obtained from Beckman Coulter (CD14, CD11c, HLADR, CD83) or Sigma (CD62p, CD61) and used at their pre-determined optimal dilutions. Background staining was established with appropriate isotype controls, and immunofluorescence was analyzed using a FC500 flow cytometer (Beckman Coulter). Two-color membrane staining was performed by adding the pre-determined optimal concentrations of both antibodies directly conjugated to FITC or PE and incubating for 20 min at 4°C, followed by washing to remove unbound antibodies. Combined membrane and cytoplasmic staining was

performed following manufacturer's instructions for cell fixation and permeabilization (Intraprep kit, Beckman Coulter).

Quantitative real-time PCR: Gene expression was compared between cells exposed during flow through the parallel plates to low (10 $\pm$ 5/low power field [lpf']) verses high (102 $\pm$ 32/lpf) levels of platelets, followed by overnight culture. Cell RNA was isolated using RNeasy Mini Kit columns with on-column DNase I treatment (QIAGEN). RNA yield and purity were measured using the NanoDrop ND-1000 Spectrophotometer and the Agilent 2100 Bioanalyzer. RNA was reverse transcribed to cDNA using the High Capacity cDNA Reverse Transcription Kit (Applied Biosystems). Reverse transcription was carried out in a 96-well thermocycler (MJ Research PTC-200) in the following conditions: 25°C, 10 minutes, 37°C, 120 minutes, 85°C, 5 seconds. TaqMan real-time PCR was used to detect transcripts of DC-LAMP, CD40, ADAM Decysin, Lox1, CCR7, CD80, CD83, CD86, FPRL2, and GPNMB. Primers and probes for each sequence were obtained as inventoried Taqman Gene Expression Assays (Applied Biosystems). HPRT1 was used as a reference gene.

Co-cultures of Platelets with Monocytes: Experiments involving co-cultures of monocytes with additional platelets were performed as described in the Overnight Culture section, with a few necessary modifications. Following Ficoll-Hypaque separation, mononuclear cells were resuspended in 30% AB serum/RMPI to a final concentration of 10 x 10^6 cells/ml, of which 1ml was allocated to each well of a 16-

well plate. An additional 1ml or platelets (suspended in RPMI, at 2x the desired end-concentration) or RPMI without platelets was then added to each well. To activate platelets, 500 μl containing 2 units of thrombin was added to half the wells, and 500 μl of RPMI was added to the others to balance volume. Cells were then incubated as described previously.

Platelet Adhesion Studies: Platelet adhesion experiments were performed using the Vena8 flow chamber described above. Fibrinogen and fibronectin (Sigma) were dissolved in PBS to a final concentration of 200 μg/ml. Channels of the Vena8 chips were incubated at room temperature in a humidified chamber for 2 hours with the protein solution, autologous plasma, or PBS alone. The channels were washed with 5x the volume RPMI. Platelet-rich-plasma was then perfused through the protein-coated channel at the indicated shear-stress, held constant. For each channel, still images were acquired exactly 90 seconds into the experiment at 4 pre-defined low power fields located along the flow path (fields were centered at 2500, 7500, 12500, and 17500 microns from the start point of infusion).

Some experiments involved pre-treating platelet-rich-plasma (PRP) with protein fragments prior to infusion through the channels. Small RGD peptides containing the amino-acid sequence Arg-Gly-Asp-Ser, DRG peptides containing the amino-acid sequence Ser-Asp-Gly-Arg, or fragment 400-411 of fibrinogen containing the amino-acid sequence His-His-Leu-Gly-Gly-Ala-Lys-Gln-Ala-Gly-Asp-Val, were incubated at

a concentration of 2mM with PRP for 20 minutes at room temperature. The PRP was then perfused through the channels as previously described.

Receptor-Ligand Studies: Same protocol followed as described in appropriate sections above, with a few necessary modifications. Vena8 platelet-coated channels were pre-treated with either 40 μg/ml anti-p-selectin (R&D Systems) or 40 μg/ml of an isotype control for 30 minutes at room temperature, then washed with 5x the volume RPMI. Mononuclear cell suspensions were pre-treated with either RGD peptides or DGR peptides at a concentration of 2.5 mM. Video samples lasting 400 frames (26.3 seconds) were recorded 60 seconds after commencement of flow using a lower power field of view spanning 400 microns and centered at 7500 microns from the flow start point.

Studies aimed at assessing the protein conformation of beta-1 integrins were conducted using the Glycotech flow chamber. 15mm platelet-coated petri dishes (as described in section above) were pre-treated with 40 μg/ml p-selectin or an isotype control for 20 minutes at room temperature, then washed with 5x the volume RPMI. Immediately following perfusion through the platelets, cells were immunophenotyped with anti-CD29 HUTS-21 (BD Biosciences), an antibody that specifically binds to the active conformation of β1 integrins.

Full-Scale-ECP: Leukocytes were collected as described above. A full-scale ECP exposure plate (Therakos) was connected in series to a peristaltic pump (MasterFlex

LS), permitting the repetitive circulation of cell-suspensions through the plate for at room temperature. When indicated, ECP exposure plates were pre-incubated with platelet-rich-plasma for 15 minutes prior to the infusion of cell-suspensions. Cell suspensions were circulated for 45 minutes at volumetric flow rates of either 100 ml/min or 24.2 ml/min, followed by 30 seconds at 280 ml/min and collection (see Appendix A). Cells were incubated overnight and phenotyped as described in the sections above.

RESULTS

Monocytes in flow transiently interact with immobilized platelets

ECP was initially developed as a means to enable extracorporeal chemotherapeutic exposure of pathogenic leukocytes to ultraviolet A (UVA)-activated 8-methoxypsoralen (8-MOP), a DNA-cross-linking drug. Therefore, ECP involves the flow of leukapheresed blood between large transparent plastic parallel-plates separated by 1 mm. To permit detailed analysis of the flow dynamics involved during ECP, independent of UVA/8-MOP exposure, we reproduced the flow conditions of ECP using miniature parallel plates with surface area of only 0.8 mm^2, separated by 100 microns. This model permitted visualization using digital microscopy. Studies using the model (see Supplement 1 for video) revealed the following sequence occurring in ECP: initial adherence of platelets from the flow stream to the plastic plate, followed by transient binding of passaged monocytes to the immobilized platelets.

DC induction correlates with the number of monocyte-platelet interactions

Based on the initial qualitative observations described above, platelets were hypothesized to contribute substantially to ECP's induction of DC. To test the influence of platelets on monocyte-to-DC differentiation, monocytes were passed between parallel plates pre-coated with autologous platelets at low (10 $\pm$ 5/low power field [lpf]), medium (44 $\pm$ 20/lpf), and high (102 $\pm$ 32/lpf) densities. The number of monocyte-platelet interactions per unit time increased in proportion to augmented density of platelets (see Supplement 2 for videos). An average of 52.3 $\pm$ 15 platelet-

monocyte interactions per lpf per second were observed with the high-density plate, dropping to 18.3 $\pm$ 14 and 3.4 $\pm$1 interactions per second with the medium and low-density plates, respectively (Figure 1A). Following overnight incubation, a correlation was found between frequency of platelet-monocyte physical interactions in the plate and the proportion of cells expressing the DC phenotype (Figure 1B). As the number of platelet-monocyte interactions increased, so too did the proportion of cells expressing markers consistent with DC differentiation, membrane HLA-DR and CD83: an average of 14.2% of monocytes exposed to the high-density platelet-coated plate were HLA-DR$^+$/ CD83$^+$ after overnight incubation, in comparison to 4.9% and 0.8% exposed to plates coated with medium and low levels of platelets, respectively.

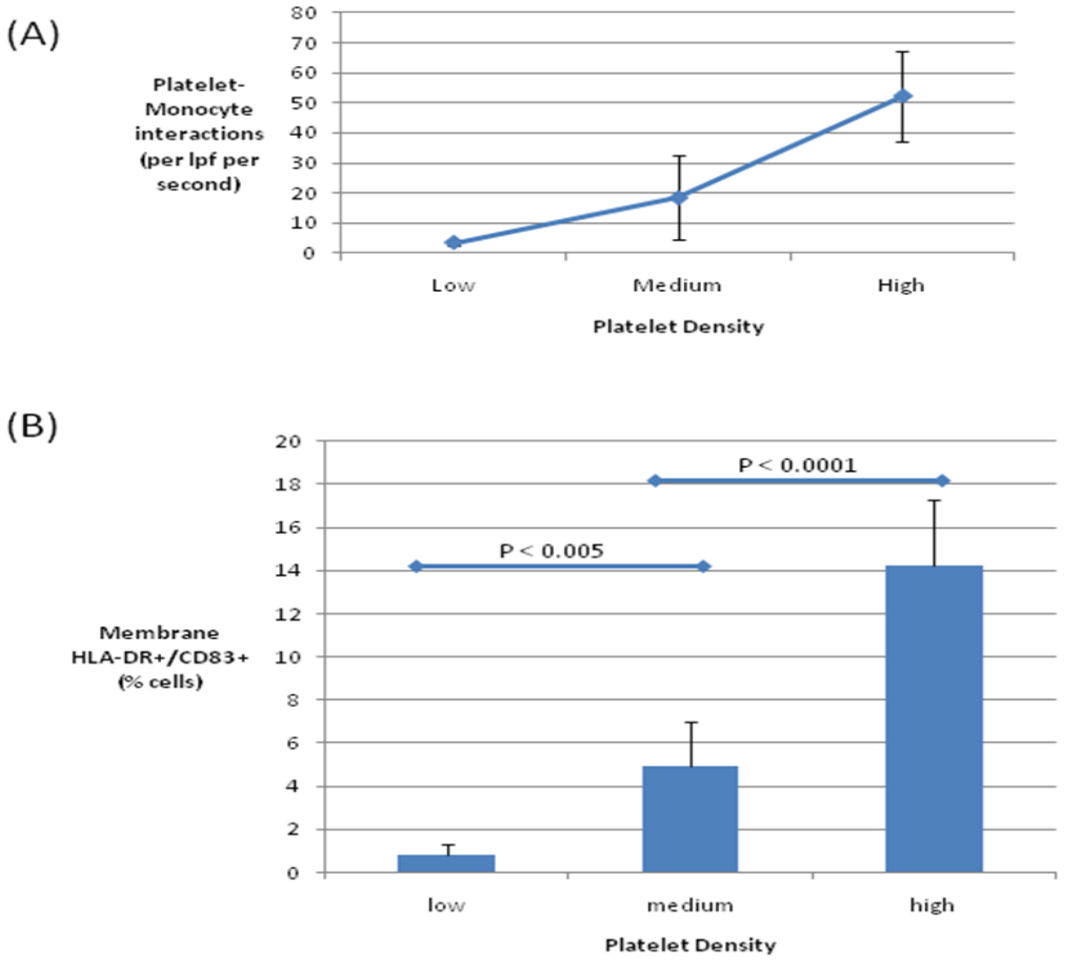

Figure 1. Effect of platelet density on number of platelet-monocyte interactions and subsequent monocyte phenotype. Monocytes were passed through parallel plates coated with platelets at low, medium, or high density. (A) The number of platelet-monocyte interactions increased substantially for plates coated with higher densities of platelets. (B) After overnight incubation, monocytes which were exposed to high levels of platelets were significantly more likely to develop a phenotype consistent with DC differentiation, as assessed by expression of membrane CD83 and HLA-DR (high versus medium or low density: $p < 0.0001$; medium versus low density: $p < 0.005$). lpf, low power field.

Monocyte exposure to platelets results in changes in gene expression

To supplement the described changes in monocyte phenotype observed following platelet exposure, RT-PCR was performed to assess for changes in gene expression. Monocytes were passed through parallel plates coated with high or low densities of platelets as described in the previous section. Following overnight incubation, RNA was extracted and RT-PCR performed to determine level of expression for 10 genes associated with DC (Figure 2). CD40, a costimulatory molecule with known expression on mature DCs [39], was found to be upregulated by over 567% in monocytes exposed to high densities of platelets relative to monocytes exposed to low levels. LAMP3, a marker specific to DC differentiation [40], was upregulated by 398%. CD80, a costimulatory molecule known to be upregulated upon APC activation [41], was found upregulated by 220% in monocytes exposed to high levels of platelets. CCR7, a chemokine receptor known to play a role in DC migration to lymphoid organs, was upregulated by 376%. LOX1, CD83, CCR7, and ADAM Decysin, all genes associated with DC [2], were upregulated in the monocytes exposed to high levels of platelets. FPRL2, GPNMB, and CD86 were all downregulated in monocytes exposed to high levels of platelets. FPRL2 is a receptor that when activated is known to inhibit DC maturation [42]; GPNMB is a protein involved in decreasing cytokine production [43]; CD86 is a costimulatory molecule expressed by APCs.

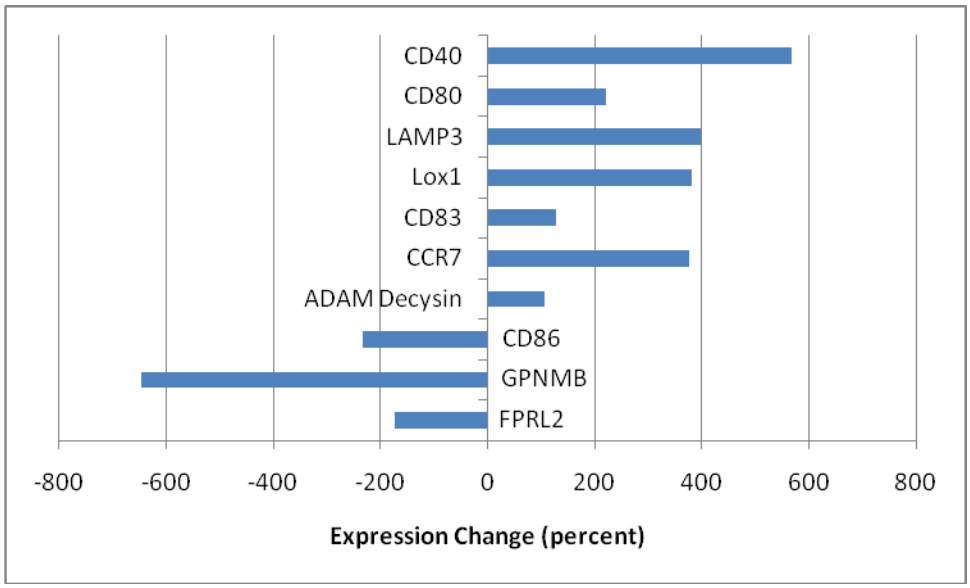

Figure 2. Gene expression following exposure to platelets. Monocytes were exposed to high or low levels of platelets in flow. Following overnight incubation, cells were assessed for differences in gene expression using RT-PCR. Figure shows gene expression changes in monocytes exposed to high levels of platelets relative to those exposed to low levels. Seven genes associated with DC-differentiation and/or function were found to be upregulated, while three were downregulated. Of the genes downregulated, GPNMB and FPRL2 have known functions in decreasing cytokine production and inhibiting DC maturation, respectively. Of the genes upregulated, all have either pro-immune functions or miscellaneous roles in DC biology. See text for specific description of genes.

DC induction did not occur under static conditions in the presence of platelets

Platelets could potentially influence monocytes through direct receptor-ligand interaction, or via cytokines and other secreted mediators. Furthermore, it is well known that formation of receptor-ligand bonds in flowing systems is influenced by shear forces [44, 45]. Accordingly, we next tested whether flow dynamics were required for platelet-dependent induction of monocytes in this system. To determine whether the platelet induction of monocyte-to-DC differentiation requires flow dynamics, we tested the role of platelets under static conditions. Monocytes were co-

cultured with low (<50,000/mm^3), medium (100-200,000/mm^3) and high (>400,000/mm^3) concentrations of platelets, with platelets in either an inactive or active state (induced by the addition of thrombin). After overnight incubation in static conditions (shear stress = 0), we found that neither activated nor non-activated platelets were capable of inducting DC differentiation of monocytes in the absence of flow (Figure 3).

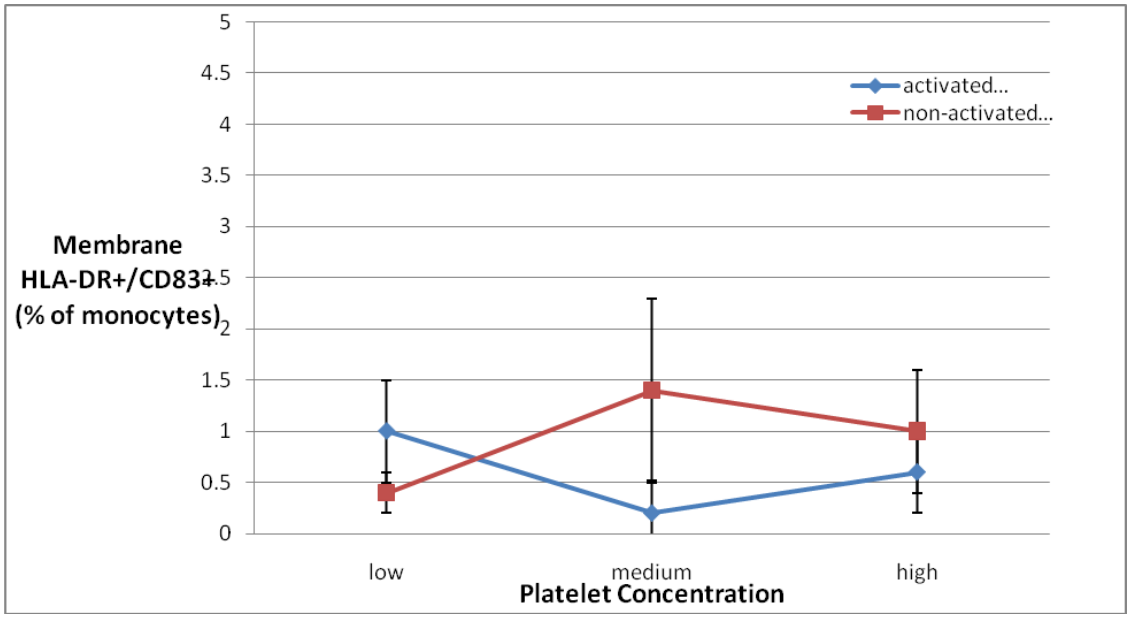

Figure 3. Platelet influence on monocyte differentiation in static conditions. Monocytes were co-cultured for 18 hours with low, medium, or high concentrations of platelets in static conditions lacking flow. Under these conditions, there was no observable platelet influence on DC differentiation; all conditions resulted in low, basline levels of cells expressing DC markers. Furthermore, activating platelets with thromin in culture (blue line) did not cause a discernable difference in monocyte differentiation relative to those cultures containing plaetlets not activated by thrombin (red line).

Platelets suspended in flow bind to serum proteins adsorbed onto the plate

A range of proteins abundantly present in plasma, including fibronectin and fibrinogen, are well known to adsorb onto glass and plastic surfaces; we therefore assessed the contribution of plastic-adherent plasma proteins on platelet adhesion and activation. Plastic parallel plates were pre-coated with either fibrinogen, fibronectin, plasma, or saline. Unactivated platelets were then passed through at shear rates producing wall shear stresses ranging from 0.2 to 6.0 dyne/cm^2 (encompassing the relevant ECP range, see Appendix A). The highest concentrations of platelets adhered to plates coated with fibrinogen (Figure 4a). Adhesion to fibronectin-coated, plasma-coated, and uncoated plates was observed as well, but to a significantly lower extent at all shear levels below 2.5 dyne/cm^2 ($p < 0.01$). In the absence of flow, platelet adherence was equivalent on all protein substrates (data not shown).

Both fibrinogen and fibronectin contain segments with the amino acid sequence arginine(R)-gylcine(G)-aspartate(D), RGD. RGD segments are well-known to interact with many integrin receptors, particularly the I/A domain of beta subunits, which are exposed when the integrins are in the active conformation [46]. In experiments using fibrinogen-coated plates, platelet adhesion was not significantly altered by pre-incubation of platelets with RGD peptides; however, adhesion was significantly decreased ($p < 0.05$) by pre-incubation of platelets with peptide fragments corresponding to amino acids 400-411 of fibrinogen, the gamma component of the protein (Figure 4b, left panel). In experiments using fibronectin-coated plates, pre-incubating platelets with RGD peptides decreased adhesion significantly ($p < 0.001$),

while pre-incubating platelets with peptide fragments corresponding to amino acids 400-411 of fibrinogen had no effect (Figure 4b, right panel). Interestingly, it should be noted that unlike the I/A domain of integrins, which is known to interact with RGD domains of proteins, the region of the intergrin found to interact with the gamma component of fibrinogen is exposed in the intergrin's *inactive* state. Therefore, this data suggests that unactivated platelets in flow bind to the gamma-component of fibrinogen-coated plates. The potential for platelets in the unactivated state to bind fibrinogen may explain the greater level of platelet adhesion seen on fibrinogen coated plates noted in the previous paragraph.

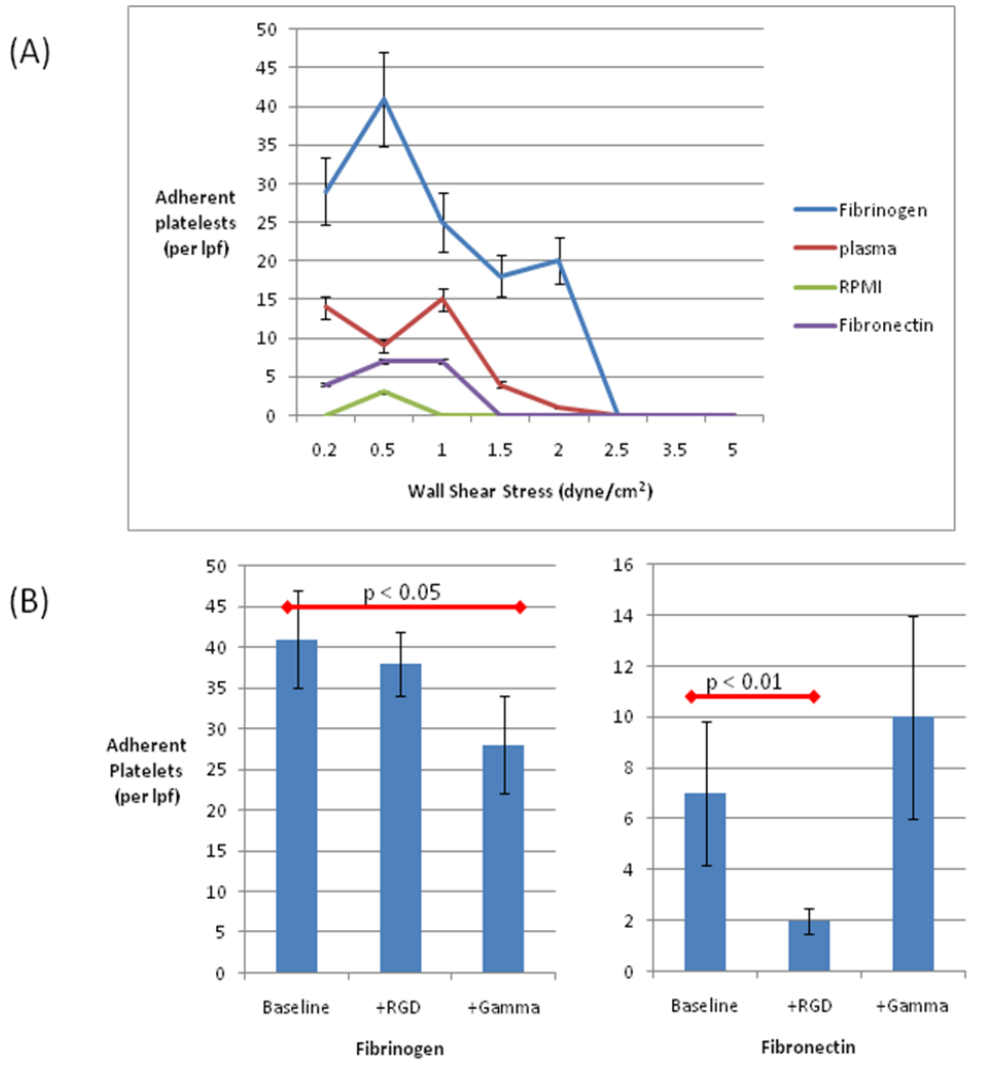

Figure 4. Plasma protein influence on platelet adhesion to plastic plates. (A) Platelets were passed through plates coated with fibrinogen (blue), plasma (red), fibronectin (purple), or RMPI (green) at the shear stress level indicated by the x-axis. Platelets in flow adhered optimally to fibronectin. For all proteins, platelet adhesion occurred maximally between 0.5 and 1.0 dyne/cm^2. (B) Platelets were pretreated with either RGD fragments (+RGD) or gamma fragments (+Gamma) and their subsequent adhesion to fibrinogen (left panel) and fibronectin (right panel) was assessed. Platelet binding to fibrinogen was decreased by gamma fragments ($p < 0.05$), while binding to fibronectin was decreased by RGD peptides ($p < 0.001$). lpf, low power field.

Platelets are activated by adhesion to the plate

Platelets physiologically circulate in an inactive state, with an array of proteins contained in intra-cellular granules, upon encountering stimuli such as damaged endothelium or thrombin, platelets become activated and translocate these intracellular proteins to the plasma membrane almost instantaneously [47]. We postulated that platelet adhesion to the plastic plate/absorbed proteins caused platelet activation similar to that caused by well-known stimuli. To test this hypothesis, we assessed surface expression of p-selectin, a well-known marker of platelet activation, before and after adhesion. Prior to adhesion, 6 $\pm$ 3% of platelets were found to express p-selectin, with a mean fluorescence intensity (MFI) of 12.4 $\pm$ 6.9; following adhesion, p-selectin positivity increased to 64 $\pm$ 13% (MFI 98.2 $\pm$ 14). The positive control consisted of platelets activated with thrombin and was found to be 71 $\pm$ 18 % p-selectin positive (MFI 108.3 $\pm$ 23). Since the clinical ECP procedure can often last longer than 60 minutes, expression of p-selectin was further assessed at 30, 60, and 90 minutes following adhesion. P-selectin expression was found to remain stable at all time points, with 72 $\pm$ 11% of platelets p-selectin positive 90 minutes after adhesion, indicating that platelets remain in an active state for the duration of the clinical procedure. Similar trends were found in assessment of αIIb-β3, a fibrinogen-binding integrin, with surface expression of this protein increasing significantly following adhesion (data not shown).

Monocytes interact with p-selectin and RGD-containing ligands expressed on activated platelets

The monocyte-platelet interactions observed on video were divided into two categories: (1) short-acting, defined as contact occurring for less than 3 seconds (48 frames), and (2) long-acting, defined as contact longer than 3 seconds, including stable binding. Since we previously determined that the platelets in the ECP system were in an activated state, and activated platelets express an array of proteins including p-selectin and RGD containing proteins (e.g.fibronectin, fibrinogen, and vitronectin), we sought to determine the involvement, if any, of these proteins in either short or long-duration interactions. Plastic plates were pre-coated with platelets, and 4 conditions tested: (1) platelets pre-treated with an irrelevant isotype control, and monocytes untreated (P+RGD+); (2) platelets pre-treated with an irrelevant isotype control, and monocytes pre-incubated with RGD peptides (P+RGD-); (3) platelets pre-treated with anti-p-selectin, and monocytes untreated (P-RGD+); (4) platelets pre-treated with anti-p-selectin, and monocytes pre-treated with RGD peptides (P-RGD-). Pre-treating monocytes with RGD peptides should result in a decreased in the number of free RGD-recognizing receptors available to interact with RGD-containing proteins expressed by the platelets. Thus, the four conditions tested represent every permutation of potential interaction with 2 platelet ligands: p-selectin and RGD-containing-proteins. As shown by Figure 5, both short-acting and long-acting interactions were maximal when neither RGD nor p-selectin were blocked (P+RGD+), and the level of interaction in all other conditions was expressed as a percentage of this maximum. Blocking with anti-p-selectin alone (P-RGD+) resulted in a decrease of both short and long monocyte-

platelet interactions to almost zero ($p < 0.01$, Figure 6, Supplements 3 for video). In contrast, blocking RGD along (P+RGD-) did not significantly alter the number of short-duration interactions, but decreased the long-duration monocyte-platelet interactions by 44% ($p < 0.05$, Figure 6). Blocking both p-selectin and RGD simultaneously (P-RGD-) resulted in a pattern similar to that seen when only p-selectin was blocked, with both long and short duration interactions reduced to near zero.

The logical conclusions which are most appropriate, based on the pattern of interactions observed in each of the four conditions, are as follows: (1) p-selectin is predominantly responsible for the short-duration interactions; (2) RGD-containing proteins expressed by the platelet are involved in long-duration interactions, but not short-duration interactions; (3) monocyte interaction with p-selectin must occur upstream of monocyte interaction with RGD-containing proteins expressed by platelets. Conclusion (3) immediately above is based on the observation that conditions of P-RGD+ decreased both short and long duration interactions to near zero, while P+RGD- conditions only influenced (decreased) long-duration interactions. If there was no sequentiality involved in the interactions, then given that P+RGD- only resulted in a decrease in long-duration interactions, conditions of P-RGD+ should have produced similar results to P+RGD+ in terms of long-duration interactions. Furthermore, the ordering of the interactions, i.e. that p-selectin acts upstream of RGD-interactions, is apparent by the finding that conditions of P+RGD- only influenced long duration interactions, while conditions of P-RGD+ produced similar results to those of P-RGD-.

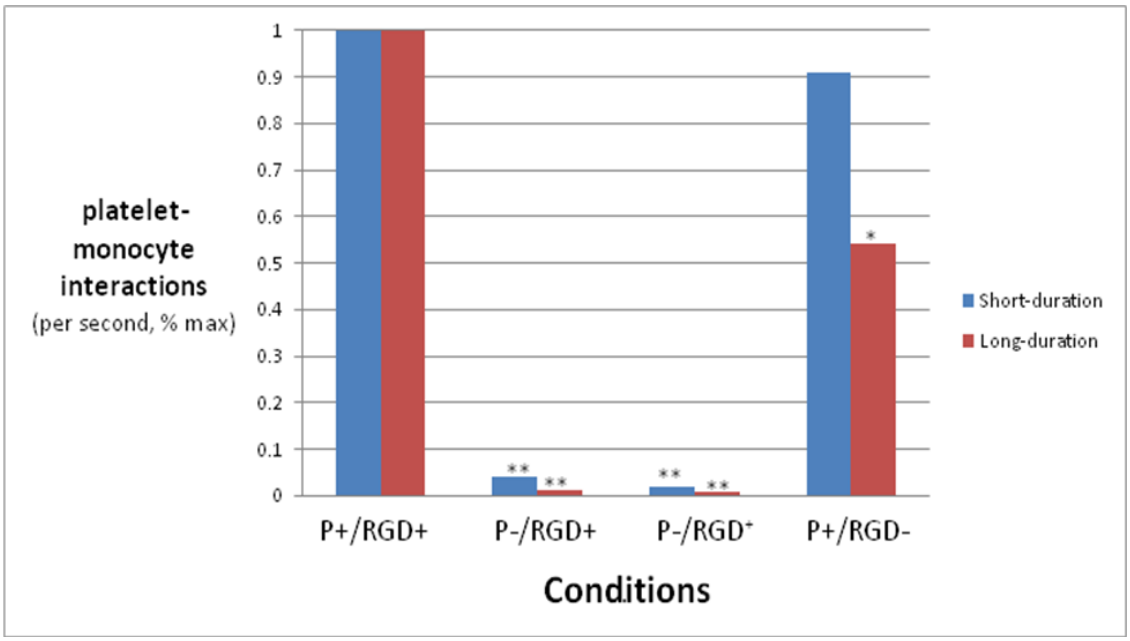

Figure 5. Proteins involved in platelet-monocyte interactions. Monocytes were passed between platelet-coated plates at a wall shear stress of 0.5 dyne/cm^2 under the conditions indicated by the x-axis: platelets were either pretreated with anti p-selectin (P-) or an isotype control (P+); monocytes were either pretreated with RGD peptides (RGD-) or a control fragment (RGD+). Platelet-monocyte interactions were quantified under each set of conditions using digital microscopy, and are expressed in the figure as a fraction of the maximum seen under conditions of P+/RGD+. Interactions were divided into those lasting less than 3 second (short duration, blue bars) and those lasting greater than 3 seconds, including stable binding (long-duration, red-bars). All conditions which involved blocking with anti-p-selectin (P-) resulted in a significant decrease in both short and long duration interactions (**, $p < 0.01$); Blocking only RGD (RGD-) resulted in a significant decrease in long-duration interactions (*, $p < 0.05$) but no change in short-duration interactions.

Monocyte exposure to P-selectin results in downstream monocyte integrin-activation

Integrin receptors, in their open conformation, are known to interact with RGD-containing ligands [48]. Using an antibody that recognizes an epitope exposed only when the β1 integrin is in its open conformation, we assessed the conformation of monocyte integrins before and after flow through the ECP model. Figure 6 shows that as the number of short-acting monocyte-platelet interactions increased, there was corresponding increase in the percentage of monocytes expressing integrins in their open conformation immediately post-flow. The blue line shows that an average of 71% of monocytes which had received a high number of platelet-interactions (> 61$\pm$ 19 /lpf x sec) expressed β1 in the active form, in comparison to 9% monocytes which received a low number of platelet interactions (< 5.1 $\pm$ 2 /lpf x sec). These results were not significantly affected by pre-treating the adherent platelets with an irrelevant isotype control (red line). In contrast, pre-treating platelets with anti-p-selectin reduced the platelet-monocyte interactions to near zero, and monocytes emerging from flow in these conditions (green line) displayed low levels of active β1 integrins, irrespective of the density of platelets to which they were exposed. It is noteworthy that all cell populations prior to passage through the plates demonstrated similar low levels (data not shown) of baseline integrin activation; therefore, differences seen in short-duration monocyte-platelet interactions were not the result of differences in integrin conformation pre-flow.

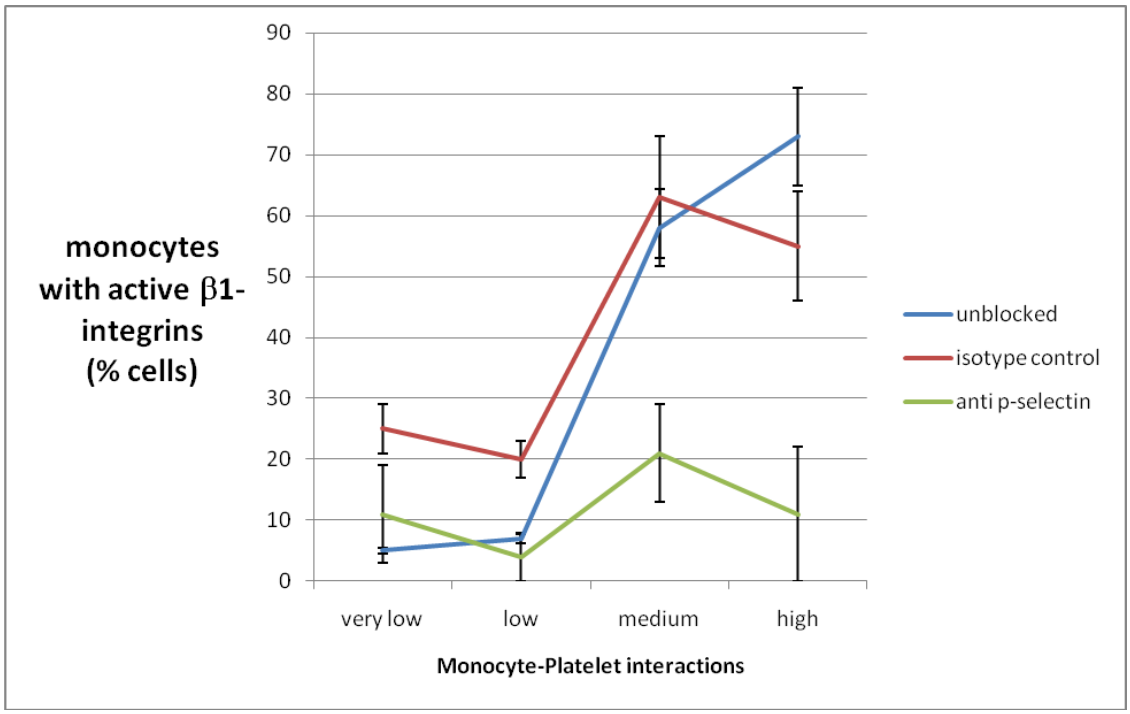

Figure 6. Effect of p-selectin exposure on monocyte intergrins. Plastic plates were coated with platelets at the relative density indicated by the x-axis. Platelets were then pretreated with anti p-selectin (green line) or an isotype control (red line), or received no pretretment (blue). Monocytes were passed through the plates at 0.5 dyne/cm^2 and then immediately assessed by flowcytometry for expression of active β1 integrins. The y-axis indicates the percent of monocyte which bound an antibody directed at an epitope only exposed when the integrin is in the open confirmation.

Monocyte exposure to P-selectin required for DC differentiation

Given the dependence of platelet-monocyte interactions on platelet p-selectin, we set out to determine if there was a relationship between monocyte exposure to p-selectin at time 0, and the phenotype later developed by the monocyte after overnight incubation, time 18-hours (Figure 7). Monocytes were passed though parallel plates coated with high densities (108 $\pm$ 36/lpf) of platelets that were either untreated (unblocked), or pretreated with either anti-p-selectin or an isotype control. On average, 15.5 $\pm$ 4 % of monocytes exposed to unblocked platelets became membrane HLA-DR$^+$/CD83$^+$

(markers of maturing DC) after overnight incubation, and 13 ± 4 % of the those exposed to platelets blocked with the irrelevant isotype control. In stark contrast, only 3 ± 2% of the those monocytes exposed to platelets blocked with anti-p-selectin became HLA-DR+/CD83+ after overnight incubation.

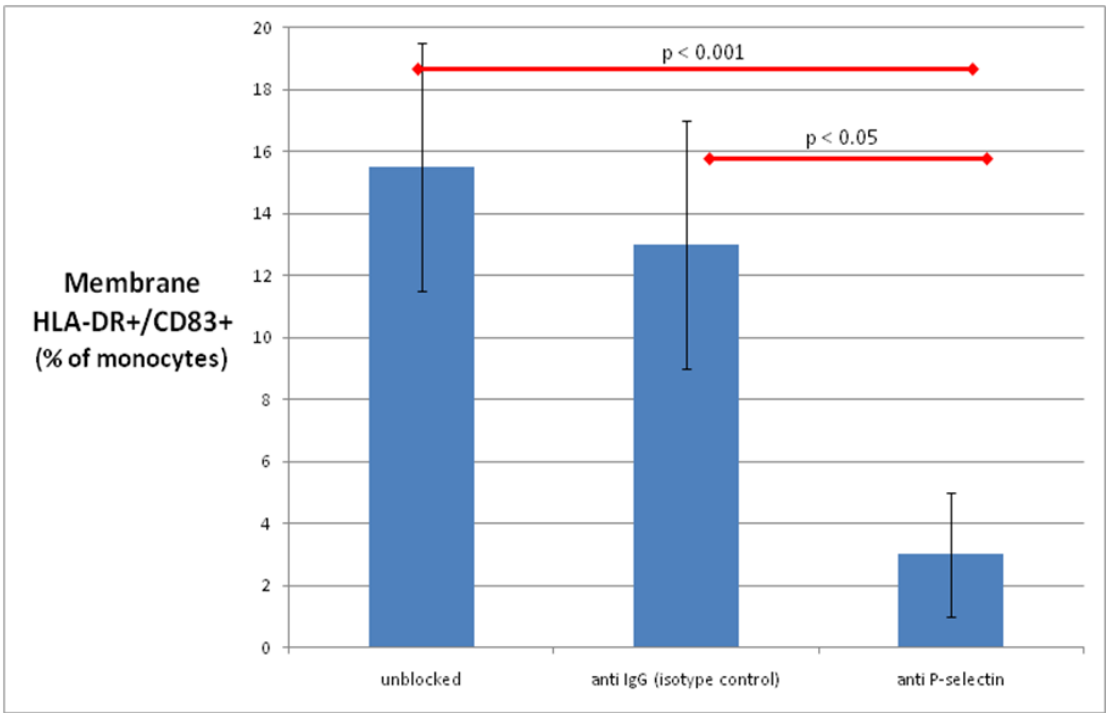

Figure 7. Effect of p-selectin exposure on monocyte phenotype after overnight incubation. Platelet-coated plates were either untreated (first column), or pretreated with an isoptype control (second column) or anti p-selectin (third column). Monocytes were passed through the plates at 0.5 dyne/cm^2 then incubated overnight. The y-axis indicates the percent of monocytes which developed a phenotype consistent with DC differentiation, membrane HLA-DR$^+$/CD83$^+$.

Enhancement of ECP's DC-generating capacity

Since our data indicate that platelets induce monocyte-to-DC differentiation, the following changes were incorporated into the traditional clinical ECP system to maximize monocyte interactions with platelets:

First, experiments and mathematical calculations determined that the optimal volumetric flow rate for maximizing monocyte-platelet interactions in the ECP apparatus was 24 ml/min (as opposed to currently used clinical value of 100 ml/min). Details pertaining to this determination can be found in Appendix A. Briefly, this value was determined by (1) experimental evidence that monocyte-platelet interactions preferentially occur at wall shear stress between 0.4-0.6, and (2) correcting for the dependence of cell flux on flow rate (see Appendix A).

Second, clinical ECP exposure plates were pre-coated with platelets.

Third, a "wash-out" step, in which elevated shear forces were applied to disassociate any platelet-attached monocytes, was applied for approximately 30 seconds at the conclusion of the ECP procedure.

Fourth, since the previously described interactions with platelets are independent of UVA energy, and indeed, all the previously described results using the model were carried out in the absence of both 8-MOP and UVA, we simplified the clinical ECP system by eliminating the use of 8-MOP and UVA energy.

Using this enhanced ECP system, 50.5 $\pm$ 11 % of the treated monocyte population was found to enter the DC pathway as determined by measuring the membrane expression

of HLA-DR and cytoplasmic CD83, compared with 30.0 ± 6% in traditional ECP, and 5.25 ± 2% of the non-treated control (Figure 8).

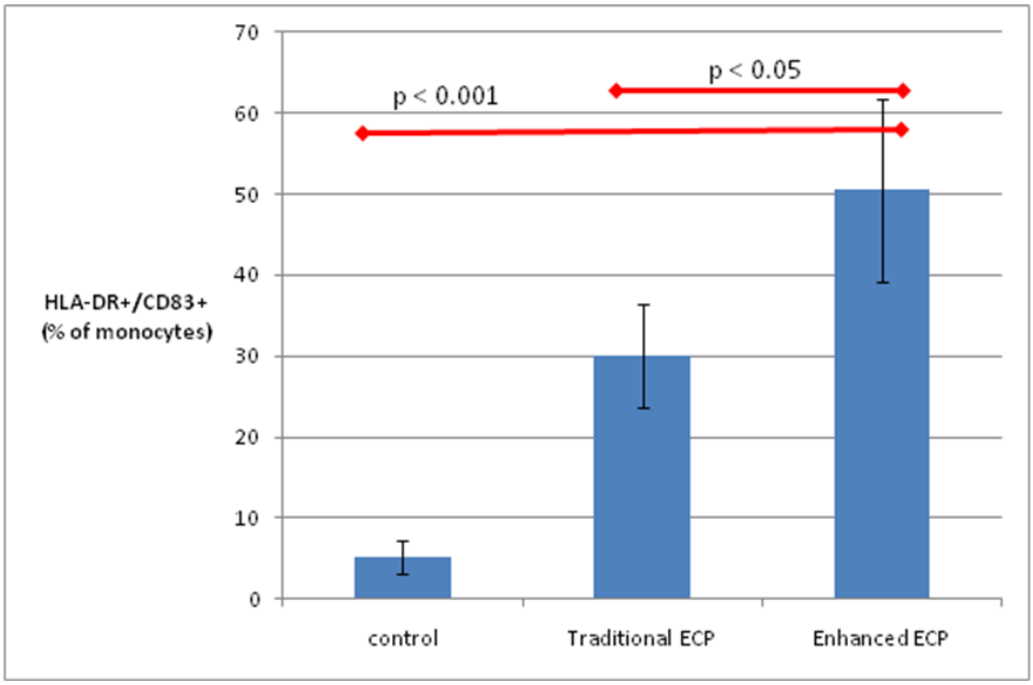

Figure 8. Enhancement of traditional ECP. The traditional ECP system was modified based on principles presented in this thesis to maximize platelet-monocyte interactions: (1) flow rate was changed from 100 ml/min to 24 ml/min; (2) exposure plate was pre-coated with platelet rich plasma; (3) theoretically adherent cells were "washed out" with application of high shear stresses at the conclusion of treatment; (4) the use of 8-MOP and UVA energy was discontinued. Each of the three conditions on the x-axis were conducted side-by-side using samples obtained from the same subject, repeated and averaged for 4 subjects. Control samples did not receive exposure to the ECP apparatus, but underwent the identical preparation steps which treated samples received.

DISCUSSION

Our collective data reveal that platelets substantially contribute to signaling the induction of monocyte-to-DC differentiation. By providing a setting in which ample monocyte-platelet interactions may occur, ECP may be co-opting and enhancing a natural physiologic mechanism for DC generation. The rapidity and efficiency of this cellular conversion, in the absence of exogenously added growth factors and without the need for lengthy tissue culture, are consistent with the timeframe and conditions normally operative in vivo in the initiation of DC responses.

Previous studies on ECP had revealed that the procedure causes large scale conversion of passaged blood monocytes into leukocytes with features typical of DC, in terms of: genetic expression, phenotype, and functional capabilities [1, 49]. This generation of DC, cells known to orchestrate the body's immune response, may be responsible for the therapy's clinical effectiveness. A lack of mechanistic knowledge regarding how ECP induced DC-differentiation has precluded introduction of scientifically-based modifications. Enhancement of the therapy could potentially expand its therapeutic scope to encompass a much broader range of cancers beyond CTCL.

Our results are consistent with the following mechanistic steps, in terms of DC generation, taking place in ECP (see Figure 9, pg 44): (1) plasma fibrinogen first coats the plastic surface of the flow chamber; (2) through its αIIbβ3 receptor, unactivated platelets bind and adhere to the plastic-immobilized fibrinogen; (3) platelets become activated and instantaneously express preformed p-selectin; (4) passaged monocytes

transiently bind p-selectin via PSGL-1, causing partial monocyte activation and integrin receptor conformational changes; (5) partially-activated monocytes, now capable of further interactions, bind additional platelet-expressed ligands, including those containing RGD domains; (6) finally, so influenced, monocytes efficiently enter the DC maturational pathway.

The above mechanism is in agreement with both our results as well as known physiologic interactions reported elsewhere. For instance, physiologically, healthy endothelium acts as an inhibitor of platelet adhesion [50, 51]; since ECP involves platelet-flow in the absence of this inhibition, it is reasonable to expect that platelets would adhere and activate upon contact with the ECP plate's surface, as we have observed.

Platelet activation is a critical step, as it opens the possibility of a number of monocyte-platelet interactions taking place within the ECP apparatus. Upon platelet activation, intracellular alpha and delta granules containing preformed proteins are translocated to the plasma membrane, and along with other mechanisms, result in the increased expression and/or secretion of an array of proteins capable of interacting with monocytes [52]. These proteins include: p-selectin, fibronectin, fibrinogen, CD40L, TNF Superfamily 14, TREM-1 ligand, IGF-1, platelet derived growth factor (PDGF), platelet factor 4 (PF4), TGF-β, thrombospondin, RANTES, and CXCL10.

In order for monocytes to receive the majority of these signals from the platelet, the monocyte must be partially activated, that is, they must have the suitable receptors expressed in the correct "open" conformation. One ligand constitutively expressed by

monocytes is PSGL-1, a proteoglycan capable of interacting with P-selectin expressed by activated platelets [53]. Our findings show that monocyte binding to platelet p-selectin resulted in monocyte integrin conformational changes, thereby allowing the monocyte to receive additional signals from the platelet downstream. Furthermore, blocking p-selectin resulted in a complete attenuation of monocyte to DC differentiation. Other studies have reported that the PSGL-1:p-selectin interaction results in increased expression and activation of the α4β1 and αMβ2 integrins [24, 25], NFκB activity [54], TNF-α secretion [54], Tissue Factor expression [55, 56], MCP-1 secretion [54, 57], and increased chemokine synthesis [58].

Downstream of p-selectin, platelet ligands containing RGD domains are likely involved in interactions with monocytes. Our results indicate that blocking RGD binding-sites results in a significant decrease in the long-duration monocyte-platelet interactions. Proteins such as fibrinogen and fibronectin contain RGD domains and are expressed by activated platelets at a high density. Monocyte integrins α5β1, αMβ2, αVβ3, αVβ1, and others are capable of binding RGD domains, with fibronectin and fibrinogen serving as principle ligands for α5β1 and αMβ2, respectively [48]. Integrin signaling is well known to affect gene expression, cell growth, activation, and survival [59].

In addition to RGD-containing proteins, other possible platelet interactions that could contribute to DC induction include CD40L with monocyte CD40. CD40L has been previously shown to serve as a potent activator of monocytes, and under the right conditions, its role appears to be equivalent to that of LPS [28, 32-34]. TNF

superfamily 14, expressed by activated platelets, has been shown to interact with monocytes and induce proinflammatory cytokine profiles, as well as cause partial DC maturation in certain settings [35-37]. TREM-1, a ligand on monocytes, is known to play a large role in LPS-induced inflammation [32, 38]; interestingly, the ligand can also engage TREM-1L expressed by activated platelets [60]. PDGF, PF4, TGF-β, RANTES, and other platelet derived products have all also been shown to induce pro-inflammatory changes in monocytes [40-44]. Additional studies will be required to clarify the potential importance of these and/or other platelet ligands in facilitating monocyte-to-DC differentiation.

The clinical success of the ECP system may very well lie in its ability to provide an in vitro environment for monocyte-platelet interactions to take place. Removing platelets from the confines of the endothelium places them in a pro-adhesive state in which they readily become activated. Furthermore, the flow component of ECP provides the natural shear forces necessary for platelet-monocyte bond formation to form. Without shear forces, bonds that evolved to form in flowing arteries and capillaries are less energetically favorable and unlikely to form [44, 45]. We found that activated platelets alone, without flow, were not sufficient to cause DC differentiation.

The rapidity and efficiency with which this induction occurs suggests a physiologic role for the mechanism. Why platelets, well known for their roles in hemostasis and thrombosis, may have evolved to play a DC-inducing role can only be speculated. It should be pointed out though, that at both the cellular and molecular levels, many similarities exist between inflammation and thrombosis. For instance, inflammation

leads to an imbalance of procoagulant to anticoagulant properties of the local endothelium, leading to platelet accumulation and activation [31-33]. Furthermore, platelets, due to the physical forces of flow and the phenomenon of radial dispersion, circulate in blood at a radial position closer to the endothelium than any white blood cell [61]. In this sense, platelets can be viewed as surveying endothelium for signs of chronic infection/inflammation. From this position, we propose that platelets are ideal for recruiting and activating a few monocytes to enter the tissue and differentiate to APC that can orchestrate the immune system's adaptive response. This pivotal role of the platelet would only add to the relatively recent body of literature placing it as a central player in numerous inflammatory processes [62-65].

The implications for potentially exploiting the mechanism described in this manuscript are tremendous. It may be possible with future advancements to generate DC for treatment of other hematologic malignancies beyond CTCL, as well as solid tumors. Furthermore, the ease with which this mechanism produces DC raises the possibility that ECP could become an attractive source of DC for other experimental protocols.

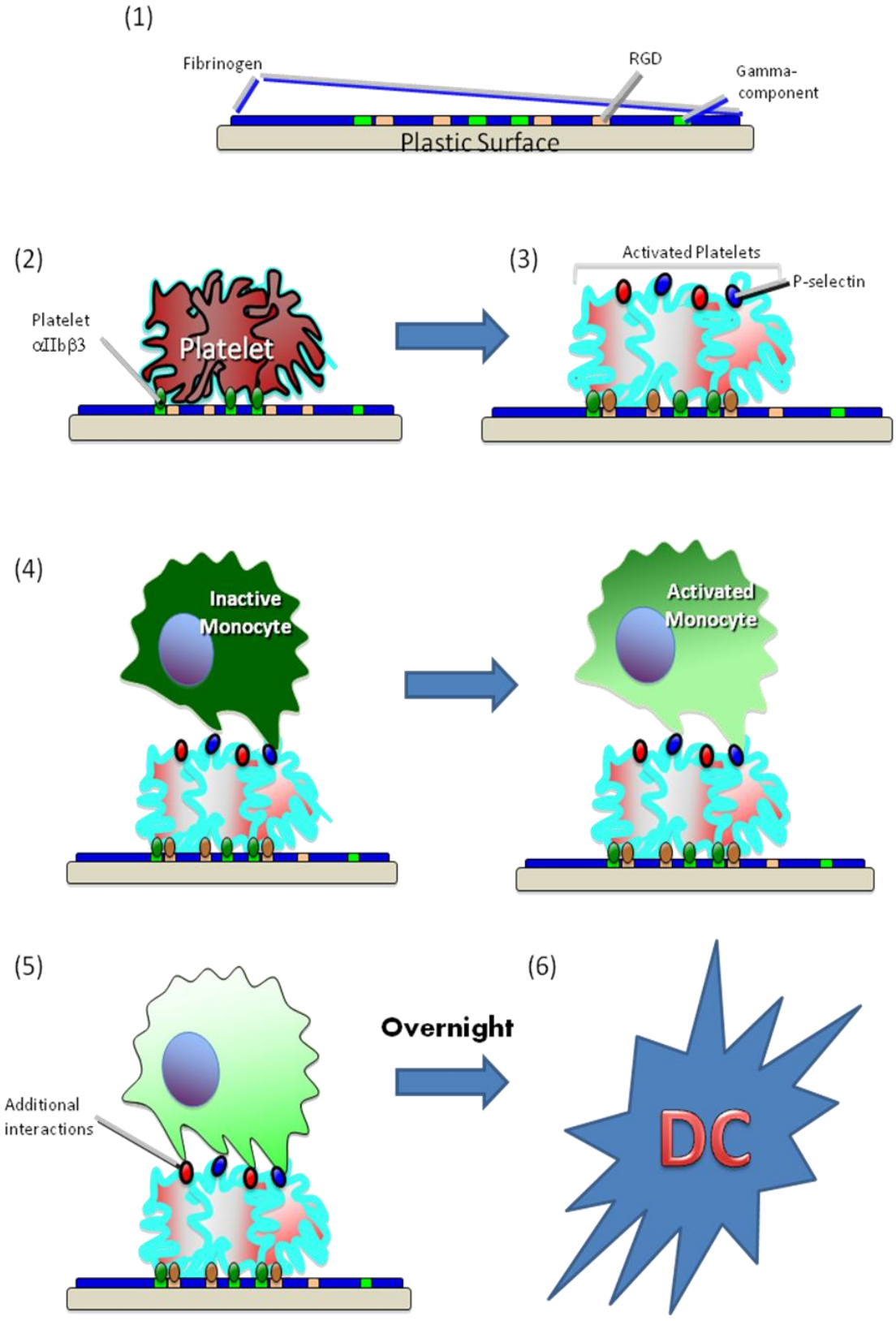

Figure 9. Proposed mechanism for induction of monocyte-to-DC differentiation. Based on data presented in this thesis, the following sequence of events are postulated: (1) plasma fibrinogen coats the plastic surface of the flow chamber; (2) through its αIIbβ3 receptor, unactivated platelets bind to the gamma-component of immobilized fibrinogen; (3) platelets become activated and instantaneously express preformed p-selectin and other proteins; (4) passaged monocytes transiently bind p-selectin via PSGL-1, causing partial monocyte activation and integrin receptor conformational changes; (5) partially-activated monocytes, now capable of further interactions, bind additional platelet-expressed ligands, including those containing RGD domains; (6) finally, so influenced, monocytes efficiently enter the DC maturational pathway within 18 hours. Note that step (1) above may be replaced physiologically by inflammatory signals from tissue acting on local endothelium, causing it to recruit and activate platelets in a similar manner (see text).

SUPPLEMENTS

Please see attached CD-ROM for access to the following supplemental material:

Supplement 1: video, initial studies using ECP model

Supplement 2: video, effect of platelet density on monocytes

Supplement 3: video, effect of anti-p-selectin on monocyte interaction with platelets

APPENDIX A

Mathematics Governing the Flow Dynamics of Extracorporeal Photochemotherapy

Overview

Initially developed as a means of exposing T-cells to specific titratable doses of UVA energy, the development of ECP coincidentally generated a system which subjected human cells to complex flow dynamics. An in-depth understanding of the mathematics governing the flow dynamics in ECP is therefore central to the development and testing of any hypothesis involving cellular interactions occurring within the ECP apparatus.

Principles key to understanding flow dynamics in ECP are derived and presented for the first time in this section, along with descriptions of how, in theory, certain easily modified ECP parameters can influence this dynamic system at the mathematical level.

Mathematically Modeling ECP

Figure A1. Therakos ECP plate.

The ECP exposure plate used clinically by the Therakos System is shown above. During a clinical ECP procedure, cells taken from the patient are repeatedly cycled

through this plate, which holds approximately 70 ml of fluid at a given time point. The plate can be described as consisting of 7 linear segments measuring 25cm (length) by 3.0 cm (width) by 0.1 cm (depth), connected by 6 regions containing a curvature of approximately 0.33 cm^{-1} (note: curvature is equal to approximately the inverse of the radius, as measured from the center of the channel). Using a Cartesian coordinate system, from this point forward this text will refer to the direction of flow as occurring in the x-direction; the z-axis existing perpendicular to the x-axis and the two greatest surfaces of the plate, and the y-axis existing perpendicular to both x and z as defined above.

As with any system involving fluids, flow will occur down a potential energy gradient as long as resistance is finite. In the case of ECP, this potential energy gradient is generated by a peristaltic pump, which for simplicity will be modeled as generating a driving force which does not vary with time.

Although the potential energy difference (i.e. driving force) is the same for all molecules, it can be hypothesized that not all molecules in flow will develop the same velocity in the steady state. Solvent molecules interact with each other through H-bonds and Van dar waals forces. The pressure difference generated by the pump in the x-direction essentially leads to a force on the molecules which opposes the inter-solvent forces. If the force generated by the pressure difference is greater than that of adhesion, rows of molecules will accelerate in the x-direction. The force generated by the pressure difference will be the same on all molecules regardless of its y-coordinate, therefore all rows of molecules will be subjected to the same profile of forces *relative*

to its neighbors, and therefore each row should develop the same acceleration and velocity *relative* to its neighbors. As Figure A2 illustrates, the equal relative velocities of one row with respect to its neighboring row generates an interesting velocity profile with respect to a common, stationary point of reference: the velocity of molecules relative to this stationary point increase as the number of rows separating the stationary point and molecule of interest increases. In the hypothetical situation depicted in Figure A2, the pressure difference generated by the ECP pump results in one row overcoming inter-molecular forces to a degree that allows it to move past its neighboring row at a velocity of 2 x-units per second. These small displacements add up, such that relative to the stationary wall, a molecule just 8 rows away will be moving at velocity of 16 x-units per second.

Figure A2. Velocity increases as distance from wall increases.

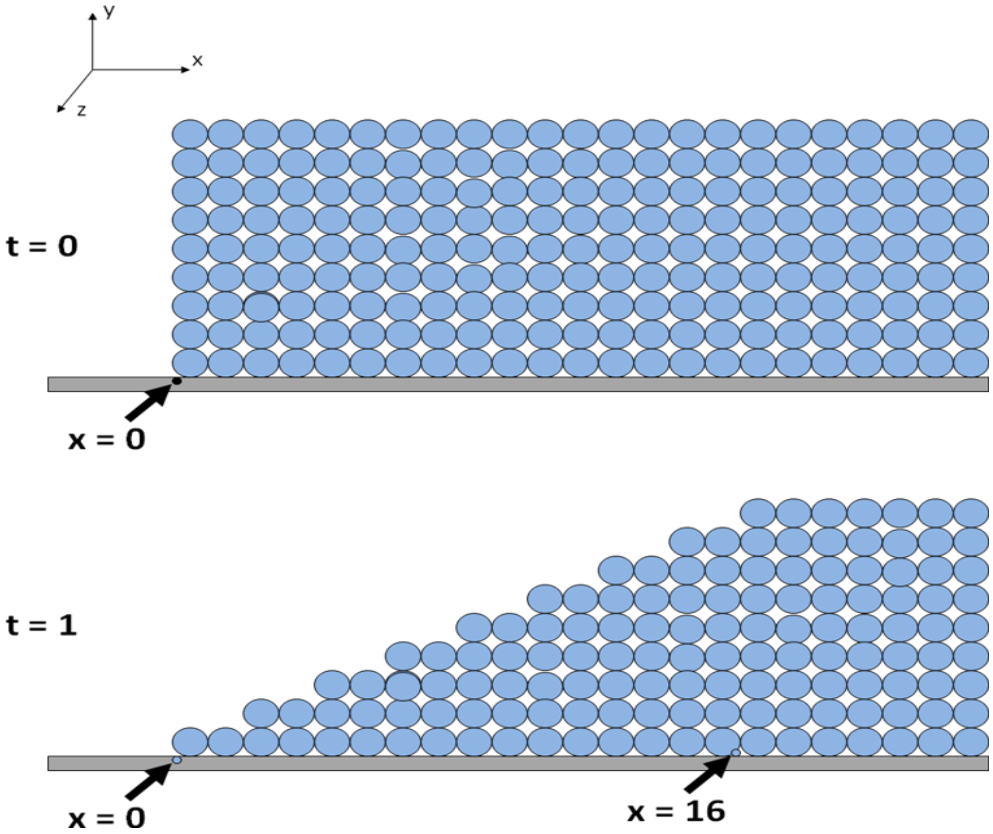

To describe the phenomena explained above and other parameters of flow in useful quantitative terms, we look to the Navier-Stokes equations for help in the derivation of parameters particular to the ECP system we are studying. Navier-Stokes equations are non-linear partial differential equations that arise from applying Newton's second law of motion to fluids; the equations describe fluid motion, and are particularly useful in the case of one-dimensional flow. Their derivation has been described elsewhere [66] and are shown below

$$\frac{\partial \rho}{\partial t}+\frac{\partial(\rho u)}{\partial x}+\frac{\partial(\rho v)}{\partial y}=0$$

$$\frac{\partial(\rho u)}{\partial t}+\frac{\partial(\rho u^2+p)}{\partial x}+\frac{\partial(\rho uv)}{\partial y}=\frac{\partial \tau_{xx}}{\partial x}+\frac{\partial \tau_{xy}}{\partial y}$$

$$\frac{\partial(\rho v)}{\partial t}+\frac{\partial(\rho uv)}{\partial x}+\frac{\partial(\rho v^2)}{\partial y}=\frac{\partial \tau_{xy}}{\partial x}+\frac{\partial \tau_{yy}}{\partial y}$$

$$\frac{\partial(\rho e+\rho\frac{u^2+v^2}{2})}{\partial t}+\frac{\partial(\rho u h_0)}{\partial x}+\frac{\partial(\rho v h_0)}{\partial y}=\frac{\partial(k\frac{\partial T}{\partial x})}{\partial x}+\frac{\partial(k\frac{\partial T}{\partial y})}{\partial y}+\frac{\partial(u\tau_{xx}+v\tau_{xy})}{\partial x}+\frac{\partial(u\tau_{xy}+v\tau_{yy})}{\partial y}$$

In the above equations: ρ = density; u and v = the Cartesian components of velocity along the x and y axes, respectively; p = pressure; T=temperature; t=time; e = specific internal energy (= internal energy per unit mass of fluid = CvT, where Cv is the specific heat at constant temperature); ho = specific total enthalpy (= total enthalpy per unit mass). Additionally, the stresses due to viscosity above, t_{xx}, t_{xy}, and t_{yy}, are related to velocity by the Stokes Relations:

$$\tau_{xx} = 2\eta\frac{\partial u}{\partial x}-\frac{2}{3}\eta\left(\frac{\partial u}{\partial x}+\frac{\partial v}{\partial y}\right)$$

$$\tau_{yy} = 2\eta\frac{\partial v}{\partial y}-\frac{2}{3}\eta\left(\frac{\partial u}{\partial x}+\frac{\partial v}{\partial y}\right)$$

$$\tau_{xy} = \eta\left(\frac{\partial u}{\partial y}+\frac{\partial v}{\partial x}\right)$$

$$\tau_{yx} = \eta\left(\frac{\partial u}{\partial y}+\frac{\partial v}{\partial x}\right)$$

Because of the nonlinear nature of the Navier-Stokes equations, exact solutions are difficult to obtain. In the case of applicability to ECP, high level of simplification can be applied to move towards exact solutions. First, we can assume that a steady state is reached which involves fully developed flow, and therefore all time derivatives in the

above equations can be removed. Second, we assume that viscosity remains constant throughout the experiments.

Third, and most importantly: as described above, the Therakos ECP plate consists of 7 linear segments connected by 6 segments with significant curvature. If we elect to only model the centers of the linear segments, far enough from the segments of curvature to assume developed flow, then Newtonian laminar flow can be assumed. In these conditions, flow occurs only in the x-direction, dropping all velocity components from the y and z-directions for the above Naiver-Stokes equations. Furthermore, since the cross-sectional dimension of linear segments, 30 mm by 1 mm, consists of a significantly greater width than depth, we assume that fluid segments behave as if the z-dimension is infinite, an assumption that only breaks down at the extremes of z. With these assumptions applied to the Naiver-Stokes equations, we obtain the following equations:

$$\frac{\partial u}{\partial x} = 0$$
$$\frac{\partial p}{\partial x} = \eta \frac{d^2 u}{dy^2}$$
$$\frac{\partial p}{\partial y} = -\rho g$$
$$\frac{\partial p}{\partial z} = 0$$

Integrating the second equation above twice with respect to y, and treating dp/dx as a constant with respect to y (as revealed by integrating the third equation above), yields:

$$u = \frac{1}{2\eta} \frac{\partial p}{\partial x} y^2 + c_1 y + c_2$$

Defining y = 0 to be the point equidistant from both plates, and defining 2h as the total distance between plates, and assuming u = 0 at y = +/- h, the coefficients for the above equation are determined to be:

$$c_1 = 0$$
$$c_2 = -\frac{h^2}{2\eta}\frac{\partial p}{\partial x}$$

Putting everything together, the velocity profile can be expressed as:

$$u = \frac{1}{2\eta}\frac{\partial p}{\partial x}\left(h^2 - y^2\right)$$

Examination of the above equation reveals that velocity is dependent on the negative square of distance from the center of the flow stream, as depicted for clarity in Figure A3. This variation is consistent with that predicted conceptually in the previous section and outlined back in Figure A2.

Figure A3. Velocity dependence on y-position

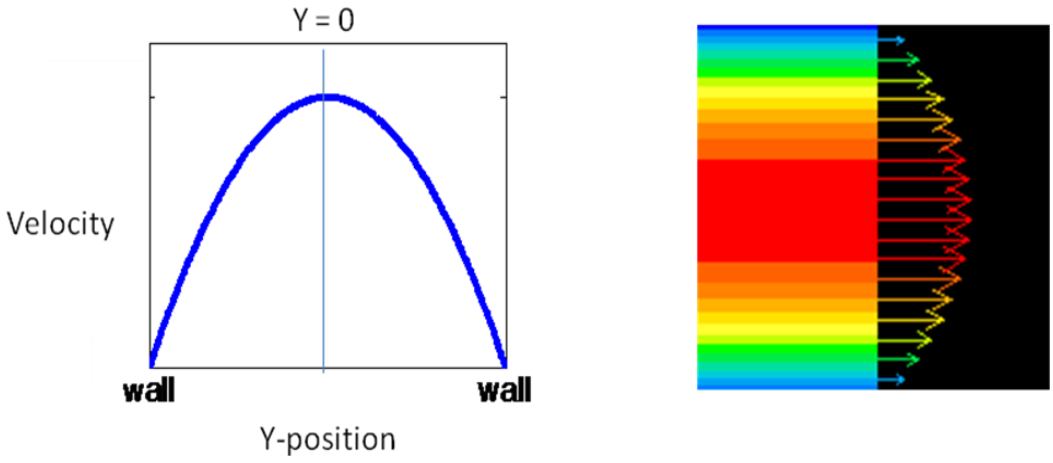

While these descriptions are helpful in understanding flow occurring in ECP, by defining a few additional parameters, these findings can be extended to help describe the complex interactions occurring between the cellular components of ECP.

Shear rate is simply the difference in velocity of one fluid layer in relation to its adjacent fluid layer, represented graphically by Figure A4, and mathematically by the subsequent equation.

Figure A4. Sheer Rate in the x direction

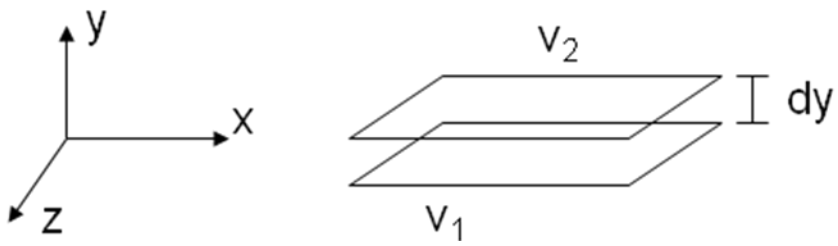

Shear Rate = $(\gamma) = \frac{v_2 - v_1}{dy} = \frac{dv_x}{dy}$

While we know the peristaltic pump in ECP generates a force driving one layer past another, Newton's second law, F=Ma, indicates that the net force must be equal to zero if the fluid is to travel at a constant velocity as it does in ECP. Therefore, an opposing force or source of energy dissipation must exist. This phenomenon is called *shear stress, τ,* and is due to molecular collisions occurring between adjacent layers. These non-elastic molecular collisions result in transfer of momentum. As can be visualized conceptually, shear stress is therefore proportional to the number of collisions

occurring per unit time, which itself is dependant on the velocity difference, or shear rate, between the two layers of fluid. Thus,

$$\tau(y) \alpha \frac{dv_x(y)}{dy}$$

This proportionality constant is referred to as fluid viscosity, η, and is dependent on composition of the fluid: the density or molecules, their molecular weight, their shape, etc. After addition of this proportionality constant, and substituting in the velocity equation worked out earlier, the shear stress can be denoted as:

$$\tau(y) = \eta \frac{d\left[\frac{1}{2\eta}\frac{\partial p}{\partial x}\left(h^2 - y^2\right)\right]}{dy} = -\frac{\partial p}{\partial x} y$$

As this equation shows, shear stress varies linearly with distance from the center of flow. Figure A5 below graphically represents and compares the y-dependence of velocity, shear rate, and shear stress.

Figure A5. Dependence of velocity, shear rate magnitude, and shear stress magnitude on y-position

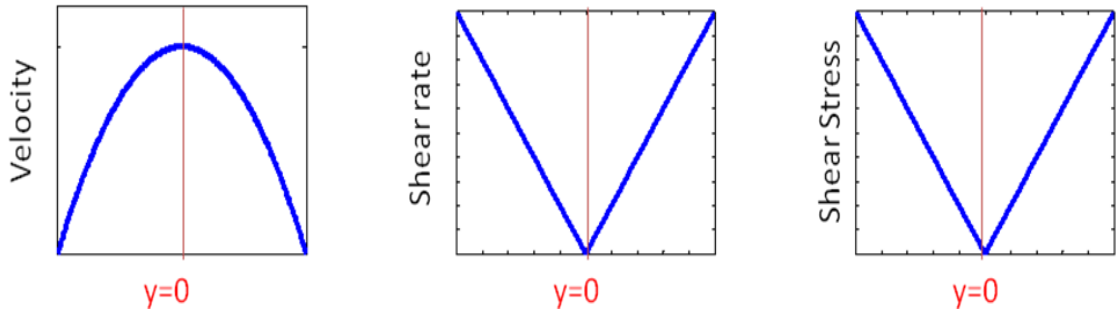

Shear stress is a parameter of critical importance in determining what bonds can form in flow [44]. Because of this importance, it was essential for us to be able to express this parameter as a function of parameters more easily described, such as volumetric flow rate, Q. In order to do this, we first recognize the conceptual association between volumetric flow rate and the velocity equation derived earlier: volumetric flow rate is the sum all volume elements passing through regions of size dydz, thus, we can obtain Q simply by integrating the velocity equation derived earlier with respect to dy and dx; this equation can then be solved for dp/dx, as follows:

$$Q = w\int_{-h}^{h} \frac{1}{2\eta}\frac{\partial p}{\partial x}\left(h^2 - y^2\right)dy = -W\frac{2h^3}{3\eta}\left(\frac{\partial p}{\partial X}\right)$$

$$\left(\frac{\partial p}{\partial X}\right) = -\frac{Q3\eta}{W2h^3}$$

Substituting this value back into shear rate equation derived above, we obtain the shear rate profile in terms of parameters easily ascertained in ECP:

$$\tau(\mathrm{y}) = \frac{Q3\eta}{W2h^3}y$$

Thus far the fluid described has consisted of simply one type of molecule, the solvent. The position of particles, or in ECP's case, white and red cells, can be ascertained by examination of the solution's shear rate dependence on y. Particles added to a solution will initially be randomly distributed, however, it can be hypothesized that theoretically once flow is initiated, particles will begin to have an increased probability of migrating towards the center of flow, or towards y = 0. This theoretical distribution is based on the likelihood that particles in solution will collide with each other, resulting in random

displacements. The number of collisions per unit time at any given distance, y, from the center of flow is dependent on the relative difference in velocity between two adjacent layers, i.e. the shear rate. Since shear rate has been calculated in the previous section to be highest near the walls and lowest at the center of flow, particles are at a greater likelihood to collide and undergo random displacements when in the periphery; should a random displacement place the particle near the center of flow, it's chances of another collision will be lower than if the random displacement places it further from the center. Thus, since the probability of receiving a random displacement is greater in the periphery than center, the flux of particles into the center will be greater than the flux out of the center. In other words, the conditions of flow in ECP will lead to the tendency of particles to undergo an organized distribution towards the center of flow.

ECP involves the flow of many cell types, including red cells, monocytes, lymphocytes, neutrophils, and platelets. These cell types have different properties such as size, density, mass, deformability, and so forth. Since the center of the laminar flow stream in ECP is a finite space, it is not possible for all cells to simultaneously reside here. To theorize on which cells will preferentially occupy this preferred region, we look to the laws of thermodynamics. It can be deduced from the laws of thermodynamics that fluids in flow look to obtain the state of least entropy, S, generation [67]. The classic definition of entropy change is simply the heat transferred divided by the temperature at which that heat was transferred, integrated from the start temperature to end temperature.

Entropy changes can be quantified in fluids without regard to temperature changes by tying together a sequence of logical statements. Since in the steady state, there is no acceleration of fluid in the x direction, all work done in the x direction must be balanced by energy dissipated by the frictional shear stress. This connects heat transfer to the previously described shear stress, which is itself connected to the work done on the fluid by the pump (since the energy transfers must be equal if the fluid is to remain at the steady state). Since work = force * distance, and distance = shear rate * dx * time, with the work of some basic algebra and integration, we can relate changes in entropy to shear stress and shear rate cleanly with the following equation:

$$\Delta S = \frac{\tau^2}{\eta} = \gamma^2 * \eta$$

This equation allows one to see that entropy changes will be proportional to the square of shear stress, which Figure A5 above shows to be a minimum at the center of flow and maximum at the walls. Therefore, entropy generation will be minimal in the state which consists of the most massive particles occupying the center of flow, where their collisions would occur at the lowest relative velocity and results in minimal energy transfer.

This principle is critical to understanding flow dynamics in ECP. It dictates that the cells with the greatest probability of interaction with the plastic plate and its absorbed proteins are those cells which are excluded from the thermodynamically preferred center of flow. Furthermore, this principle allows one to better predict, based on principle, the influence that changing ECP parameters may have on cellular

interactions. For instance, with all other parameters held constant, increasing hematocrit may paradoxically increase the number of white-cell interactions occurring at the plate wall. This is because an increasing density of red cells would in-effect better exclude white cells from the center of flow, pushing them to the periphery. Additionally, with all other parameters held constant, increasing shear rate to certain levels could decrease the number of white-cell interactions at the plastic wall for reasons other the dependence of these interactions on shear stress. Individual red cells are significantly smaller than lymphocytes and granulocytes, however, under low to medium range shear rates, red cells are known to aggregate with one-another, forming stacks of red cells known as rouleaux. These bodies are significantly greater in size and mass compared to white cells, and therefore are energetically favorable in the center of flow compared to white cells. When shear rates extend to beyond that of a critical value (dependent on other variables), the intercellular interactions maintaining these red cell formations are overcome, and the cells become individual entities. In these conditions, white cells are larger and more massive, and therefore become the cell more energetically favorable for occupation of the center of flow.

Enhancing ECP

As evident from the explained derivations, the above equations and concepts hold for any flow system consisting of constant volumetric flow between parallel plates with the z-dimension significantly larger than the y-dimension. It is therefore fairly easy to compare results and model flow conditions in one system with another.

In order to enhance the flow conditions of ECP to maximize platelet-monocyte interactions, we first recognized that the number of platelet-monocyte interactions per unit time (I_t) is the product of both the likelihood that a monocyte will interact with a platelet if within binding distance (PCT), and the flux of monocytes which are placed within a binding distance per unit time (Q_a^b). PCT is a function of shear stress, as revealed in the results section. Shear stress derived earlier can be written as a function of only Q when y is appropriately set equal h (wall shear stress). In summary, platelet-monocyte interactions per unit time can be written as:

$$I_T(Q) = Q_a^b(Q) * PCT(\tau(Q))$$

$PCT(\tau(Q))$ can be obtained using the experimental data presented in the results section on the platelet-monocyte interaction dependence on wall shear stress, extrapolated to have Q represent the necessary flow rate in the Therakos system (using equation derived earlier). $Q_a^b(Q)$ can be calculated theoretically by integrating the appropriate equations presented earlier over a theoretical binding distance. In this manner, $I_T(Q)$ is calculated to be at a theoretical maximum for the Therakos system when Q = 24 ml/min.

REFERENCES

1. Berger, C.L., et al., *Induction of human tumor-loaded dendritic cells.* International Journal of Cancer, 2001. **91**(4): p. 438-447.
2. Berger, C., et al., *Rapid generation of maturationally synchronized human dendritic cells: contribution to the clinical efficacy of extracorporeal photochemotherapy.* Blood, 2010. **116**(23): p. 4838-4847.
3. Ardavin, C., et al., *Origin and differentiation of dendritic cells.* Trends in Immunology, 2001. **22**(12): p. 691-700.
4. Hart, D.N.J., *Dendritic cells: Unique leukocyte populations which control the primary immune response.* Blood, 1997. **90**(9): p. 3245-3287.
5. Fong, L. and E.G. Engleman, *Dendritic cells in cancer immunotherapy.* Annual Review of Immunology, 2000. **18**: p. 245-273.
6. Ridgway, D., *The first 1000 dendritic cell vaccinees.* Cancer Investigation, 2003. **21**(6): p. 873-886.
7. Schuler, G., B. Schuler-Thurner, and R.M. Steinman, *The use of dendritic cells in cancer immunotherapy.* Current Opinion in Immunology, 2003. **15**(2): p. 138-147.
8. Shortman, K. and S.H. Naik, *Steady-state and inflammatory dendritic-cell development.* Nature Reviews Immunology, 2007. **7**(1): p. 19-30.
9. Geissmann, F., *Development of monocytes, macrophages, and dendritic cells.* Science, 2010. **330**(6009): p. 1318-1318.
10. Wan, H. and M. Dupasquier, *Dendritic cells in vivo and in vitro.* Cell Mol Immunol, 2005. **2**(1): p. 28-35.
11. Taylor, P.R. and S. Gordon, *Monocyte heterogeneity and innate immunity.* Immunity, 2003. **19**(1): p. 2-4.
12. Dunay, I.R., et al., *Gr1(+) inflammatory monocytes are required for mucosal resistance to the pathogen Toxoplasma gondii.* Immunity, 2008. **29**(2): p. 306-317.
13. Robben, P.M., et al., *Recruitment of Gr-1(+) monocytes is essential for control of acute toxoplasmosis.* Journal of Experimental Medicine, 2005. **201**(11): p. 1761-1769.
14. Serbina, N.V., et al., *Monocyte-mediated defense against microbial pathogens.* Annual Review of Immunology, 2008. **26**: p. 421-452.
15. Shechter, R., et al., *Infiltrating Blood-Derived Macrophages Are Vital Cells Playing an Anti-inflammatory Role in Recovery from Spinal Cord Injury in Mice.* Plos Medicine, 2009. **6**(7).
16. Geissmann, F., et al., *Blood monocytes: distinct subsets, how they relate to dendritic cells, and their possible roles in the regulation of T-cell responses.* Immunology and Cell Biology, 2008. **86**(5): p. 398-408.
17. Sallusto, F. and A. Lanzavecchia, *EFFICIENT PRESENTATION OF SOLUBLE-ANTIGEN BY CULTURED HUMAN DENDRITIC CELLS IS MAINTAINED BY GRANULOCYTE-MACROPHAGE COLONY-STIMULATING FACTOR PLUS INTERLEUKIN-4 AND DOWN-REGULATED BY TUMOR-NECROSIS-FACTOR-ALPHA.* Journal of Experimental Medicine, 1994. **179**(4): p. 1109-1118.
18. Geissmann, F., et al., *Transforming growth factor beta 1 in the presence of granulocyte/macrophage colony-stimulating factor and interleukin 4, induces differentiation of human peripheral blood monocytes into dendritic Langerhans cells.* Journal of Experimental Medicine, 1998. **187**(6): p. 961-966.

19. Chomarat, P., et al., *IL-6 switches the differentiation of monocytes from dendritic cells to macrophages.* Nature Immunology, 2000. **1**(6): p. 510-514.
20. Stein, M., et al., *INTERLEUKIN-4 POTENTLY ENHANCES MURINE MACROPHAGE MANNOSE RECEPTOR ACTIVITY - A MARKER OF ALTERNATIVE IMMUNOLOGICAL MACROPHAGE ACTIVATION.* Journal of Experimental Medicine, 1992. **176**(1): p. 287-292.
21. Martinez, F.O., et al., *Macrophage activation and polarization.* Frontiers in Bioscience, 2008. **13**: p. 453-461.
22. Edelson, R., et al., *TREATMENT OF CUTANEOUS T-CELL LYMPHOMA BY EXTRACORPOREAL PHOTOCHEMOTHERAPY - PRELIMINARY-RESULTS.* New England Journal of Medicine, 1987. **316**(6): p. 297-303.
23. Hivelin, M., et al., *Extracorporeal photopheresis: From solid organs to face transplantation.* Transplant Immunology, 2009. **21**(3): p. 117-128.
24. Marshall, S.R., *Technology Insight: ECP for the treatment of GvHD - can we offer selective immune control without generalized immunosuppression?* Nature Clinical Practice Oncology, 2006. **3**(6): p. 302-314.
25. Babic, A.M., *Extracorporeal photopheresis: Lighting the way to immunomodulation.* American Journal of Hematology, 2008. **83**(7): p. 589-591.
26. Berger, C.L., et al., *INHIBITION OF AUTOIMMUNE-DISEASE IN A MURINE MODEL OF SYSTEMIC LUPUS-ERYTHEMATOSUS INDUCED BY EXPOSURE TO SYNGENEIC PHOTOINACTIVATED LYMPHOCYTES.* Journal of Investigative Dermatology, 1990. **94**(1): p. 52-57.
27. Ovali, E., et al., *Active immunotherapy for cancer patients using tumor lysate pulsed dendritic cell vaccine: a safety study.* Journal of Experimental & Clinical Cancer Research, 2007. **26**(2): p. 209-214.
28. von Hundelshausen, P. and C. Weber, *Platelets as immune cells - Bridging inflammation and cardiovascular disease.* Circulation Research, 2007. **100**(1): p. 27-40.
29. Wagner, D.D. and P.C. Burger, *Platelets in inflammation and thrombosis.* Arteriosclerosis Thrombosis and Vascular Biology, 2003. **23**(12): p. 2131-2137.
30. Katoh, N., *Platelets as versatile regulators of cutaneous inflammation.* Journal of Dermatological Science, 2009. **53**(2): p. 89-95.
31. Yamamoto, K., et al., *Regulation of murine protein C gene expression in vivo: Effects of tumor necrosis factor-alpha, interleukin-1, and transforming growth factor-beta.* Thrombosis and Haemostasis, 1999. **82**(4): p. 1297-1301.
32. Kirchhofer, D., et al., *ENDOTHELIAL-CELLS STIMULATED WITH TUMOR-NECROSIS-FACTOR-ALPHA EXPRESS VARYING AMOUNTS OF TISSUE FACTOR RESULTING IN INHOMOGENOUS FIBRIN DEPOSITION IN A NATIVE BLOOD-FLOW SYSTEM - EFFECTS OF THROMBIN INHIBITORS.* Journal of Clinical Investigation, 1994. **93**(5): p. 2073-2083.
33. Loscalzo, J., *Nitric oxide insufficiency, platelet activation, and arterial thrombosis.* Circulation Research, 2001. **88**(8): p. 756-762.
34. Henn, V., et al., *CD40 ligand on activated platelets triggers an inflammatory reaction of endothelial cells.* Nature, 1998. **391**(6667): p. 591-594.
35. Lindemann, S., et al., *Activated platelets mediate inflammatory signaling by regulated interleukin 1 beta synthesis.* Journal of Cell Biology, 2001. **154**(3): p. 485-490.

36. von Hundelshausen, P., et al., *RANTES deposition by platelets triggers monocyte arrest on inflamed and atherosclerotic endothelium.* Circulation, 2001. **103**(13): p. 1772-1777.
37. Myers, D., et al., *New and effective treatment of experimentally induced venous thrombosis with anti-inflammatory rPSGL-Ig.* Thrombosis and Haemostasis, 2002. **87**(3): p. 374-382.
38. Nurden, A.T., et al., *Platelets and wound healing.* Frontiers in Bioscience, 2008. **13**.
39. Cella, M., et al., *Ligation of CD40 on dendritic cells triggers production of high levels of interleukin-12 and enhances T cell stimulatory capacity: T-T help via APC activation.* Journal of Experimental Medicine, 1996. **184**(2): p. 747-752.
40. de Saint-Vis, B., et al., *A novel lysosome-associated membrane glycoprotein, DC-LAMP, induced upon DC maturation, is transiently expressed in MHC class II compartment.* Immunity, 1998. **9**(3): p. 325-336.
41. Slavik, J.M., J.E. Hutchcroft, and B.E. Bierer, *CD80 and CD86 are not equivalent in their ability to induce the tyrosine phosphorylation of CD28.* Journal of Biological Chemistry, 1999. **274**(5): p. 3116-3124.
42. Kang, H.K., et al., *The synthetic peptide Trp-Lys-Tyr-Met-Val-D-Met inhibits human monocyte-derived dendritic cell maturation via formyl peptide receptor and formyl peptide receptor-like 2.* Journal of Immunology, 2005. **175**(2): p. 685-692.
43. Ripoll, V.M., et al., *Gpnmb is induced in macrophages by IFN-gamma and lipopolysaccharide and acts as a feedback regulator of proinflammatory responses.* Journal of Immunology, 2007. **178**(10): p. 6557-6566.
44. Chen, S.Q. and T.A. Springer, *Selectin receptor-ligand bonds: Formation limited by shear rate and dissociation governed by the Bell model.* Proceedings of the National Academy of Sciences of the United States of America, 2001. **98**(3): p. 950-955.
45. Thomas, W.E., *Understanding the counterintuitive phenomenon of catch bonds.* Current Nanoscience, 2007. **3**: p. 63-83.
46. Xiong, J.P., et al., *Crystal structure of the extracellular segment of integrin alpha V beta 3 in complex with an Arg-Gly-Asp ligand.* Science, 2002. **296**(5565): p. 151-155.
47. Kaplan, K.L., et al., *PLATELET ALPHA-GRANULE PROTEINS - STUDIES ON RELEASE AND SUBCELLULAR-LOCALIZATION.* Blood, 1979. **53**(4): p. 604-618.
48. Ruoslahti, E., *RGD and other recognition sequences for integrins.* Annual Review of Cell and Developmental Biology, 1996. **12**: p. 697-715.
49. Berger, C.L. and R.L. Edelson, *Rapid Generation of Maturationally Synchronized Human Dendritic Cells: Contribution to the Clinical Efficancy of Extracorporeal Photochemotherapy* Blood, 2010.
50. Macdonald, P.S., M.A. Read, and G.J. Dusting, *SYNERGISTIC INHIBITION OF PLATELET-AGGREGATION BY ENDOTHELIUM-DERIVED RELAXING FACTOR AND PROSTACYCLIN.* Thrombosis Research, 1988. **49**(5): p. 437-449.
51. Stamler, J., et al., *N-ACETYLCYSTEINE POTENTIATES PLATELET INHIBITION BY ENDOTHELIUM-DERIVED RELAXING FACTOR.* Circulation Research, 1989. **65**(3): p. 789-795.
52. Blockmans, D., H. Deckmyn, and J. Vermylen, *Platelet actuation.* Blood Reviews, 1995. **9**(3): p. 143-156.
53. Evangelista, V., et al., *Platelet/polymorphonuclear leukocyte interaction: P-selectin triggers protein-tyrosine phosphorylation-dependent CD11b/CD18 adhesion: Role of PSGL-1 as a signaling molecule.* Blood, 1999. **93**(3): p. 876-885.

54. Weyrich, A.S., et al., *MONOCYTE TETHERING BY P-SELECTIN REGULATES MONOCYTE CHEMOTACTIC PROTEIN-1 AND TUMOR-NECROSIS-FACTOR-ALPHA SECRETION - SIGNAL INTEGRATION AND NF-KAPPA-B TRANSLOCATION.* Journal of Clinical Investigation, 1995. **95**(5): p. 2297-2303.
55. Celi, A., et al., *P-SELECTIN INDUCES THE EXPRESSION OF TISSUE FACTOR ON MONOCYTES.* Proceedings of the National Academy of Sciences of the United States of America, 1994. **91**(19): p. 8767-8771.
56. Lindmark, E., T. Tenno, and A. Siegbahn, *Role of platelet P-selectin and CD40 ligand in the induction of monocytic tissue factor expression.* Arteriosclerosis Thrombosis and Vascular Biology, 2000. **20**(10): p. 2322-2328.
57. Gawaz, M., et al., *Activated platelets induce monocyte chemotactic protein-1 secretion and surface expression of intercellular adhesion molecule-1 on endothelial cells.* Circulation, 1998. **98**(12): p. 1164-1171.
58. Weyrich, A.S., et al., *Activated platelets signal chemokine synthesis by human monocytes.* Journal of Clinical Investigation, 1996. **97**(6): p. 1525-1534.
59. Giancotti, F.G. and E. Ruoslahti, *Transduction - Integrin signaling.* Science, 1999. **285**(5430): p. 1028-1032.
60. Haselmayer, P., et al., *TREM-1 ligand expression on platelets enhances neutrophil activation.* Blood, 2007. **110**(3): p. 1029-1035.
61. Kao, S.-S., *Rheology*
in *Thrombosis and hemorrhage*, J. Loscalzo, Schafer, A., Editor 2003, Lippincott Williams & Wilkins.
62. Boilard, E., et al., *Platelets Amplify Inflammation in Arthritis via Collagen-Dependent Microparticle Production.* Science. **327**(5965): p. 580-583.
63. DeSanctis, G.T., et al., *Reduction of allergic airway responses in P-selectin-deficient mice.* Journal of Applied Physiology, 1997. **83**(3): p. 681-687.
64. Huo, Y.Q., et al., *Circulating activated platelets exacerbate atherosclerosis in mice deficient in apolipoprotein E.* Nature Medicine, 2003. **9**(1): p. 61-67.
65. Massberg, S., et al., *A critical role of platelet adhesion in the initiation of atherosclerotic lesion formation.* Journal of Experimental Medicine, 2002. **196**(7): p. 887-896.
66. Temam, R., *Navier-Stokes Equations: theory and nymerical analysis*1977, New York: American Mathematical Society.
67. GF, N., *Entropy-based design and analysis of fluids engineering systems*2008, Boca Raton: CRC Press.